Food Control 189 (2026) 112334

Contents lists available at ScienceDirect

Food Control

journal homepage: www.elsevier.com/locate/foodcont

A sustainable biocontrol strategy using *Priestia aryabhattai* C-KT-3 to manage postharvest nutmeg black rot caused by *Lasiodiplodia theobromae*

Julalak Chuprom [a], Sawai Boukaew [b,*], Wanida Petlamul [b], Mongkolphet Kaewnah [b], Oanchittha Pora [b], Jirayu Buatong [c], Benjamas Cheirsilp [d], Siriporn Yossan [e], Kanokphorn Sangkharak [f], Laksanara Khwanchum [a,g], Zhiwei Zhang [h]

[a] School of Languages and General Education, Walailak University, Nakhon Si Thammarat, 80160, Thailand
[b] Faculty of Agricultural Technology, Songkhla Rajabhat University, Songkhla, 90000, Thailand
[c] International Center of Excellence in Seafood Science and Innovation, Prince of Songkla University, Hat Yai, Songkhla, 90110, Thailand
[d] Center of Excellence in Innovative Biotechnology for Sustainable Utilization of Bioresources, Faculty of Agro-Industry, Prince of Songkla University, Hat Yai, Songkhla, 90110, Thailand
[e] Division of Environmental Science, Faculty of Liberal Arts and Science, Sisaket Rajabhat University, Sisaket, 33000, Thailand
[f] Faculty of Agricultural Technology, Phuket Rajabhat University, Phuket, 83000, Thailand
[g] Center of Excellence in Sustainable Disaster Management, Walailak University, Nakhon Si Thammarat, 80160, Thailand
[h] Institute of Materia Medica, Xinjiang University, Urumqi 830017, People's Republic of China

ARTICLE INFO

Keywords:
Lasiodiplodia theobromae
Priestia aryabhattai
Secondary metabolites
Oxidative stress
Postharvest biocontrol
Nutmeg fruit

ABSTRACT

Lasiodiplodia theobromae is a major postharvest pathogen causing nutmeg black rot and was identified as the causal agent in Thailand, representing the first report in the country. Among 25 rhizosphere bacterial isolates, *Priestia aryabhattai* C-KT-3 exhibited the strongest antifungal activity *in vitro*, significantly reducing fungal growth in a concentration-dependent manner. *In vivo* assays showed that both culture filtrates and bacterial cells reduced disease severity without adversely affecting fruit quality. These results demonstrate that C-KT-3 exhibits significant antifungal activity under both *in vitro* and fruit conditions. Genome analysis revealed multiple biosynthetic gene clusters, suggesting metabolic potential, while LC–QTOF–MS profiling indicated a chemically diverse set of putative metabolites. Biochemical assays suggested the induction of oxidative stress responses in the pathogen following treatment. Overall, these findings indicate that multiple mechanisms may contribute to the observed antifungal activity and highlight C-KT-3 as a promising biocontrol agent for postharvest nutmeg disease management.

1. Introduction

Nutmeg (*Myristica fragrans* Houtt.) is a dioecious, evergreen tropical spice tree native to the Moluccas Islands of Indonesia (Biju et al., 2021). It is now widely cultivated across tropical regions, including Indonesia, Grenada, Sri Lanka, India, China, Malaysia, Western Sumatra, Zanzibar, Mauritius, the Solomon Islands, and southern Thailand. In Thailand, nutmeg is mainly grown in Phatthalung, Nakhon Si Thammarat, and Trang provinces, where it contributes significantly to local agriculture and spice production (Keereekoch et al., 2018). The crop has diverse uses, including traditional medicine, essential oil production, and as a culinary spice, making it economically valuable for both culinary and medicinal purposes.

Despite its economic importance, nutmeg production is constrained by postharvest diseases. *Lasiodiplodia theobromae* is a major pathogen responsible for black fruit rot, causing significant losses in both yield and quality (Yang et al., 2021), which affects market value and limits local and international trade. This pathogen also causes fruit rot in other economically important fruits worldwide, including mango (Gariba et al., 2025; Kaewkrajay & Dethoup, 2024), jackfruit (de Souza et al., 2024), avocado (Chen et al., 2024), fig (*Ficus carica*) (Nur-Shakirah et al., 2022), longan (Chen et al., 2021), dragon fruit (Briste et al., 2022), apple (Che et al., 2015), and banana (Salaemae et al., 2022).

Management of postharvest fungal diseases has traditionally relied on chemical fungicides such as thiabendazole, imazalil, and azoxystrobin (Mannaa et al., 2025). However, repeated use of a limited

* Corresponding author.
E-mail address: sawai.bo@skru.ac.th (S. Boukaew).

https://doi.org/10.1016/j.foodcont.2026.112334
Received 14 February 2026; Received in revised form 30 April 2026; Accepted 24 May 2026
Available online 25 May 2026

number of active ingredients increases the risk of pathogen resistance, poses health and environmental hazards, and may result in chemical residues in harvested fruits (Mora-Aguilera et al., 2021). Growing consumer concern over chemical residues has increased pressure to reduce or eliminate fungicide use in fruit and vegetable production (Pusey et al., 1993).

Beneficial microorganisms have been successfully employed as biocontrol agents to control postharvest diseases in various crops (Gava et al., 2022; Li, Li, et al., 2024; Mannaa et al., 2025; Zhong et al., 2025). These microorganisms suppress pathogens through multiple mechanisms, including the production of antibiotics, lytic enzymes, and volatile organic compounds (VOCs) (García-Montelongo et al., 2023; Nehra et al., 2022), competition for space and nutrients in the rhizosphere (García-Montelongo et al., 2023), and induction of systemic resistance in host plants. Several genera, including *Bacillus* (Li, Li, et al., 2024; Saucedo-Bazalar et al., 2023), *Paraburkholderia* (Mannaa et al., 2025), *Streptomyces* (Kamil et al., 2018), *Brevibacillus* (Che et al., 2015), and various yeasts (Gava et al., 2022), have shown effectiveness against *Lasiodiplodia* spp., helping reduce yield losses and maintain fruit quality.

Although these beneficial microorganisms are effective, their performance is influenced by factors such as geographical location, soil type, cropping system, and environmental conditions. Therefore, continuous isolation and characterization of locally adapted antagonistic strains are essential to identify robust candidates for reliable postharvest disease control. To achieve environmentally friendly management of fruit rot, this study aimed to (i) isolate and identify antagonistic bacteria from rhizosphere soil and evaluate their inhibitory activity against *L. theobromae*, (ii) elucidate the mechanisms underlying the biocontrol effects of the selected strain, and (iii) assess the biological characteristics of *Priestia aryabhattai* C-KT-3 and its potential to preserve postharvest nutmeg quality.

2. Materials and methods

2.1. Sample collection, morphological characteristics, and pathogenicity test

Naturally infected nutmeg fruits exhibiting disease symptoms were collected from orchards managed by the Baan Suan Chan Community Enterprise Group for Nutmeg Product Processing (8.193139° N, 99.845305° E), located in Ron Phibun Subdistrict, Ron Phibun District, Nakhon Si Thammarat Province, Thailand. Symptomatic nutmeg fruits showing necrotic lesions and internal discoloration were collected for laboratory analysis. Peel tissues were surface-sterilized by immersion in 1% sodium hypochlorite for 30 s, rinsed with sterile distilled water for an additional 30 s, and air-dried under aseptic conditions. Tissue segments (~0.5 cm), excised from the interface between diseased and healthy areas, were placed onto potato dextrose agar (PDA; HiMedia™) and incubated at 28 ± 2 °C. Fungal colonies became visible within 3 days, after which the predominant isolate was purified through successive subculturing and single-spore isolation following Chomnunti et al. (2014). The resulting isolate, designated NM-01, was used for morphological characterization and subsequent analyses.

The fungal strain NM-01 was characterized based on its morphological features. Colony morphology was examined on PDA plates after incubation at 28 ± 2 °C for 3 and 10 days, and at 35 °C for 5 days. The formation of pycnidia, mycelium, and spores was assessed after 30 days of incubation. Mycelium and spores from 30-day-old cultures of NM-01 were mounted in lactophenol cotton blue (HiMedia, Maharashtra, India) on clean glass slides and examined under a light microscope (ZEISS Primostar 3, Jena, Germany). Micrographs were captured, and conidial dimensions were measured using ZEN microscopy software.

Pathogenicity of the isolated fungus was evaluated using healthy, freshly harvested nutmeg fruits. Before inoculation, fruits were surface-disinfected by sequential immersion in 70% ethanol, 1% sodium hypochlorite, and sterile distilled water for 30 s each. A single shallow wound was then made on each fruit using a sterile needle. The fungal conidial suspension was prepared in sterile distilled water containing 0.03% (v/v) Tween 20 and adjusted to 1×10^7 spores/mL. Subsequently, 5 μL of the suspension was carefully deposited onto each wound site. Inoculated fruits were placed individually in sterile plastic containers (19.2 × 28.0 × 10.9 cm^3) and incubated at 28 ± 2 °C under high relative humidity (90–95%). Symptom development was monitored and documented by photography at 6 days after inoculation. The pathogen was subsequently re-isolated from infected nutmeg tissues to fulfill Koch's postulates.

2.2. Molecular identification of fungal isolate NM-01

The fungal pathogen NM-01 was identified by phylogenetic analysis based on the internal transcribed spacer (ITS) region and large subunit (LSU) rRNA gene sequences. Both gene regions were amplified and sequenced by Macrogen Co., Ltd. (Seoul, South Korea) using the primer pairs ITS5 (5′-GGA AGT AAA AGT CGT AAC AAG G-3′) and ITS4 (5′-TCC TCC GCT TAT TGA TAT GC-3′) for the ITS region, and LR0R (5′-ACC CGC TGA ACT TAA GC-3′) and LR7 (5′-TAC TAC CAC CAA GAT CT-3′) for the LSU rRNA gene. The obtained sequences were compared with reference sequences in the GenBank database using the Basic Local Alignment Search Tool (BLAST) (http://www.ncbi.nlm.nih.gov/BLAST/Blast.cgi) to assess sequence homology.

Phylogenetic trees based on ITS and LSU sequences were constructed using the MEGA 12 program with neighboring species to confirm the taxonomic placement of NM-01 within the genus *Lasiodiplodia*. The evolutionary history was inferred using the Maximum Likelihood method. The analysis was conducted under the following parameters: the General Time Reversible (GTR) substitution model, Gamma distribution with invariant sites (G + I) for rate variation among sites, and five discrete gamma categories. The reliability of the tree topology was evaluated using the bootstrap method with 1000 replications. All sites, including gaps and missing data, were included in the analysis, and the initial tree was automatically generated using the NJ/BioNJ approach.

2.3. Soil samples collection and bacteria isolation

Bacterial isolates were obtained from the collected soil samples using a standard protocol (Küster & Williams, 1964). A total of five rhizosphere soil samples were collected from chili plants (*Capsicum annuum* L.) at various sites in Ko Taeo Subdistrict (7.092140° N, 100.622502° E), Mueang Songkhla District, Songkhla Province, Thailand. One gram of each soil sample was suspended in 9 mL of sterile saline solution (0.85% NaCl) and shaken on a rotary shaker at 150 rpm at 28 ± 2 °C for 24 h. Subsequently, 1 mL of the suspension was transferred into 9 mL of sterile saline solution in a 15-mL microtube and serially diluted up to 10^{-7}. Aliquots of 0.1 mL from the 10^{-5} to 10^{-7} dilutions were spread onto nutrient agar (NA; HiMedia™) plates and incubated at 37 °C. After 5 days of incubation, morphologically distinct colonies were picked and streaked onto fresh NA plates for purification. Pure cultures were maintained on NA slants at 4 °C for further use.

2.4. Screening of antagonistic bacteria against L. theobromae in vitro

2.4.1. Dual culture effect

All bacterial strains were evaluated for their antagonistic activity against *L. theobromae* using a dual-culture assay (Mannaa et al., 2025). Each bacterial strain was grown in 5 mL of nutrient broth (NB; HiMedia™) and incubated on a rotary shaker at 150 rpm and 37 °C for 24 h. The resulting cell suspension was adjusted to approximately 10^7 CFU/mL. A loopful of each bacterial culture was streaked onto one side of a NA plate and incubated at 37 °C for 24 h to allow sufficient bacterial growth. After incubation, a 5-mm-diameter mycelial plug taken from a 3-day-old *L. theobromae* colony was placed on the opposite side of the NA plate, approximately 5 cm away from the bacterial streak. For the control treatment, a mycelial plug of *L. theobromae* was placed on an

uninoculated NA plate. All plates were incubated at 28 ± 2 °C for 3 days. The radial growth of *L. theobromae* toward the bacterial colony (treatment) and on the control plates was measured. The percentage of radial growth inhibition was calculated using the following formula: Inhibition (%) = [(Control − Treatment)/Control] × 100. Each treatment was performed in triplicate and repeated twice.

2.4.2. Volatile organic compounds effect

The sealed plate assay was employed to assess the *in vitro* antifungal activity of VOCs produced by ten selected bacterial isolates against *L. theobromae* (Calvo et al., 2020). A 5-mm-diameter agar plug taken from the actively growing margin of a 3-day-old *L. theobromae* colony on PDA was placed at the center of a PDA plate. In parallel, NA plates were inoculated with 100 μL of a 24-h bacterial culture adjusted to approximately 10^7 CFU/mL. The two base plates were joined face-to-face and sealed with Parafilm™ to prevent VOCs leakage. PDA plates containing only *L. theobromae* (without bacterial VOCs exposure) served as the control. All plates were incubated at 28 ± 2 °C for 3 days. The colony diameter of *L. theobromae* was measured, and the percentage of mycelial growth inhibition was calculated as previously described. Each treatment was performed in triplicate and repeated twice.

2.5. Whole-genome sequencing, taxonomic identification, and analysis of secondary metabolite biosynthetic gene clusters in C-KT-3

The whole genome of C-KT-3 was sequenced using an Illumina platform. Clean reads were *de novo* assembled using Unicycler (Wick et al., 2017). Gene prediction and annotation were performed using PROKKA for protein-coding sequences (CDSs), tRNAscan-SE v2.0 for transfer RNA (tRNA) genes, and Barrnap for ribosomal RNA (rRNA) genes (Seemann, 2014).

For phylogenomic analysis, the whole-genome sequence of C-KT-3, together with 20–30 publicly available genomes of closely related *Priestia* species, was analyzed using the AutoMLST2 web server. Genome FASTA files were processed through the *de novo* workflow, in which pairwise genomic distances were first estimated based on Mash and average nucleotide identity (ANI), followed by the selection of the closest reference genomes from the GTDB database. Conserved single-copy marker genes shared among all included taxa were subsequently identified, individually aligned, and concatenated into a single supermatrix. A maximum-likelihood phylogenomic tree was inferred using IQ-TREE under the best-fitting substitution model selected by AutoMLST2, based on the concatenated core-gene alignment. Branch support was evaluated using 1000 bootstrap replicates. The resulting Newick-format tree was exported and visualized in FigTree v1.4.4, and the terminal labels were edited to indicate the corresponding species or strain names along with their genome accession numbers.

Secondary metabolite–associated biosynthetic gene clusters (BGCs) in C-KT-3 were predicted using antiSMASH v6.0.1. The identified BGCs were annotated and compared with characterized clusters deposited in the MIBiG database. Similarity levels (high, medium, or low) were assigned based on concordance in gene content and overall cluster architecture, as reported by the antiSMASH output.

2.6. Antifungal activity of C-KT-3 culture filtrates against L. theobromae

The antifungal activity of C-KT-3 culture filtrates (CFs) was evaluated under solid (PDA) and liquid (potato dextrose broth, PDB; HiMedia™) conditions. C-KT-3 was cultured in NB at 37 °C for 48 h with shaking at 150 rpm. The culture was centrifuged at 8880 × g for 15 min, and the supernatant was filtered through a 0.22 μm membrane to obtain sterile CFs.

For the PDA assay, CFs were incorporated into double-strength PDA to obtain final concentrations of 1–60% (v/v). A 5-mm mycelial plug of *L. theobromae* was placed at the center of each plate and incubated at 28 ± 2 °C for 3 days. The colony diameter of *L. theobromae* was measured, and the percentage of mycelial growth inhibition was calculated as previously described.

For the PDB assay, CFs were added to PDB to achieve final concentrations of 1–60% (v/v). Each flask was inoculated with a spore suspension (1×10^7 spores/mL), followed by incubation at 150 rpm, 28 ± 2 °C, for 3 days. After incubation, mycelial biomass was collected, dried at 60 °C, and weighed to determine fungal dry weight. The percentage of growth inhibition was calculated using the following equation: Inhibition (%) = $[(W_1 - W_2)/W_1] \times 100$, where W_1 is the dry biomass of the untreated control and W_2 is that of CFs-treated samples. All treatments were performed in triplicate and repeated twice.

2.7. Comparative efficacy of C-KT-3 culture filtrates, commercial fungicides, and preservatives against L. theobromae

Five commercial fungicides were used in this study: thiram (80% WG), propiconazole (25% w/v), azoxystrobin (25% w/v), prochloraz (45% w/v), and metalaxyl (25% WP). These products are commonly used in agricultural practice and are readily available in Thailand. Stock formulations were diluted to final concentrations of 0.1–0.8% (v/v), based on their respective active ingredient (a.i.) contents.

Two food-grade preservatives, sodium benzoate and sodium propionate, were obtained from Aldrich (Milwaukee, WI, USA). Sodium benzoate, approved by the FDA as a food preservative, is typically used at concentrations between 0.05% and 0.1% (w/v) (Jay, 1992), while sodium propionate is generally applied at 0.1% to 0.2% (w/v). Both preservatives were dissolved in sterile distilled water to prepare concentrations of 0.05%, 0.1%, 0.15%, and 0.2% (w/v).

The antifungal efficacy of C-KT-3 CFs (60% v/v) was compared with that of commercial fungicides (0.1–0.8% v/v) and preservatives (0.05–0.2% w/v) on PDA. Each concentration of C-KT-3 CFs, fungicides, and preservatives was incorporated into molten PDA (45–50 °C) to a total volume of 10 mL per plate. A 5-mm-diameter agar plug taken from the actively growing margin of a 3-day-old *L. theobromae* colony on PDA was placed at the center of each treated plate and incubated at 28 ± 2 °C for 3 days. PDA plates without any additives served as controls. The colony diameter of *L. theobromae* was measured, and the percentage of mycelial growth inhibition was calculated as previously described. Each treatment was performed in triplicate and repeated twice.

2.8. Broad-spectrum antifungal activity of C-KT-3 culture filtrates against plant pathogenic fungi

The broad-spectrum antifungal activity of C-KT-3 CFs was evaluated against ten plant pathogenic fungi: *Schizophyllum commune, Rhizoctonia solani, Peniophora salaccae, Curvularia oryzae, Aspergillus parasiticus, Aspergillus flavus, Sclerotium rolfsii, Corynespora cassiicola, Colletotrichum musae,* and *Fusarium incarnatum*. Based on previous results, 60% (v/v) CFs was selected for evaluation in PDB. Each fungus was inoculated into PDB supplemented with CFs, while PDB without CFs served as the control. Cultures were incubated at 28 ± 2 °C under shaking conditions (150 rpm) for 3–7 days depending on fungal growth rate. Mycelial biomass was determined after drying, and growth inhibition was calculated as previously described. Each treatment was performed in triplicate and repeated twice.

2.9. LC–QTOF–MS-based identification of antifungal metabolites in culture filtrates of C-KT-3

Antifungal metabolites in C-KT-3 CFs were analyzed using LC–QTOF–MS (Agilent 1290 Infinity II LC coupled with 6545 Q-TOF, Agilent Technologies, USA). Chromatographic separation was performed on a C18 column (150 × 2.1 mm, 1.8 μm) at 25 °C using a gradient of 0.1% acetic acid in water and methanol at a flow rate of 0.2 mL/min. The injection volume was 10 μL. Mass spectrometric analysis was conducted in both positive and negative electrospray ionization

modes (+ESI and –ESI) using AutoMS/MS acquisition. Data were collected over *m/z* 100–1200, and compounds were putatively identified by matching accurate masses and fragmentation patterns with the METLIN database using MassHunter software (Agilent Technologies).

2.10. Evaluation of C-KT-3 efficacy in controlling nutmeg black rot and maintaining fruit quality

2.10.1. Evaluation of C-KT-3 efficacy in controlling nutmeg black rot

The biocontrol efficacy of C-KT-3 against nutmeg black rot was evaluated using CFs and bacterial cell suspensions. Uniform and disease-free nutmeg fruits were prepared following the procedure described in the previous subsection and subjected to a wound-inoculation assay. Fruits were first inoculated with a *L. theobromae* spore suspension (1×10^7 spores/mL), and then CFs (25–100% v/v) or cell suspensions (10^5–10^8 CFU/mL) were applied to the same wound sites. Treated fruits were incubated at 28 ± 2 °C and 90–95% relative humidity. After 5 days of incubation, disease severity was assessed by measuring lesion diameter on each fruit. Disease control efficiency was calculated as the percentage reduction in lesion size compared with the untreated control using the following equation: Disease control (%) = [(L_control − L_treatment)/L_control] × 100, where L_control is the mean lesion diameter of the control and L_treatment is that of the treated fruits. Each treatment was replicated three times, with six fruits per replicate, resulting in a total of 18 fruits per treatment.

2.10.2. Evaluation of the effects of NM-01 inoculation and C-KT-3 treatment on nutmeg fruit quality

Following disease evaluation, nutmeg fruits subjected to different treatments were further analyzed for postharvest quality attributes. Fruit juice was obtained by homogenizing the pulp and filtering through cheesecloth to remove solid residues. The effects of CFs and cell suspensions of C-KT-3 at different concentrations were evaluated based on multiple postharvest quality parameters, including.

2.10.2.1. Determination of total soluble solid content. Total soluble solids (TSS) were determined using a refractometer and expressed as °Brix, following standard procedures described by AOAC International (2019) for fruit and juice samples. Each treatment was performed in triplicate and repeated twice.

2.10.2.2. Determination of total titratable acidity. Total titratable acidity (TTA) was determined by acid–base titration using phenolphthalein as an indicator, following AOAC International (2019) with slight modifications (Li, Zhang, et al., 2024). Samples were homogenized prior to analysis. TTA was expressed as % (w/v) citric acid and calculated based on the volume of standardized 0.1 N NaOH, with correction for the reagent blank, using the following equation: TTA (%) = $[(A_1 - A_2) \times N \times 0.064 \times 100]/V$, where A_1 is the volume of NaOH used for the sample (mL), A_2 is the blank volume (mL), N is the normality of NaOH, and V is the sample volume (mL). Each treatment was performed in triplicate and repeated twice.

2.10.2.3. Determination of total phenolic contents. Total phenolic content (TPC) was determined using the Folin–Ciocalteu colorimetric method, following Limcharoen et al. (2022). Briefly, samples were mixed with diluted Folin–Ciocalteu reagent and sodium bicarbonate solution, and incubated at room temperature for 1 h. Absorbance was measured at 765 nm using a microplate reader (Thermo Scientific, Göteborg, Sweden). A calibration curve was constructed using gallic acid (4–30 μg/mL), and the results were expressed as mg gallic acid equivalents per gram of extract (mg GAE/g). Each treatment was performed in triplicate and repeated twice.

2.10.2.4. Determination of free radical scavenging activities. Free radical scavenging activity was determined using the DPPH assay, based on a modified method reported by Baliyan et al. (2022). Samples were mixed with 0.1 mM DPPH solution prepared in methanol and incubated in the dark at room temperature for 30 min. Absorbance was measured at 517 nm using a microplate reader (BioTek Synergy H1, Agilent Technologies, Winooski, VT, USA). Ascorbic acid was used as a positive control. Radical scavenging activity was expressed as percentage inhibition and calculated using the following equation: %RSA = [(A_control − A_sample)/A_control] × 100. Each treatment was performed in triplicate and repeated twice.

2.11. Mycolytic activity and antifungal mechanisms of C-KT-3

To investigate the potential mechanisms underlying the antagonistic activity of C-KT-3 against *L. theobromae*, a series of assays were conducted as follows.

2.11.1. Mycolytic activity

The ability of C-KT-3 to utilize *L. theobromae* mycelial biomass as a nutrient source and support bacterial growth was evaluated following Mannaa et al. (2023). Fungal mycelia were obtained from PDB cultures, washed, and used as a substrate. Bacterial suspensions were prepared from overnight cultures and adjusted to OD600 = 0.6. The assay was conducted in diluted NB (1:1000 v/v), with treatments consisting of C-KT-3 in the presence or absence of fungal mycelia. Each reaction contained 6 mg of fungal biomass and 100 μL of bacterial suspension and was incubated at 37 °C with shaking at 150 rpm for 2 days. Bacterial populations were quantified by plating serial ten-fold dilutions (10^0 to 10^{-5}) on NA and expressed as CFU/mL after 2 days of incubation at 37 °C. Each treatment was performed in triplicate and repeated twice.

2.11.2. Oxidative stress–related mechanism

To elucidate the antifungal mechanism of C-KT-3 CFs against *L. theobromae*, fungal mycelia were exposed to CFs as described below. Mycelial plugs were cultured in PDB for 3 days, harvested, and resuspended in fresh PDB containing 60% (v/v) CFs, while untreated samples served as controls. After an additional 3 days of incubation, mycelia were collected for biochemical analyses. Fungal biomass was homogenized in phosphate-buffered saline (100 mM, pH 7.4) and centrifuged, and the supernatant was used for subsequent assays. Reactive oxygen species (ROS) levels were determined using the DCFH-DA assay (Keston & Brandt, 1965). Catalase (CAT) activity was measured following Beers and Sizer (1952), and superoxide dismutase (SOD) activity was determined using the method of Kostyuk and Potapovich (1989). Glutathione (GSH and GSSG) contents were quantified fluorometrically according to Kostyuk and Potapovich (1989). Protein content was determined by the Lowry method (Lowry et al., 1951). Enzyme activities were expressed per mg protein. All treatments were performed in triplicate and the experiment was repeated twice.

2.12. Statistical analysis

All experimental data were analyzed using IBM SPSS Statistics 26 (IBM Corp., Armonk, NY, USA). Data were tested for normality and homogeneity of variance prior to analysis. One-way analysis of variance (ANOVA) followed by Tukey's HSD test was used to evaluate differences among multiple treatments ($p < 0.05$). For pairwise comparisons between each treatment and the untreated control, independent samples t-tests were performed ($p < 0.05$). Asterisks indicate significant differences between treated samples and the untreated control within each isolate.

3. Results

3.1. Sample collection, disease symptoms, morphological characteristics, and pathogenicity test

Representative disease symptoms (Fig. 1A), morphological characteristics (Fig. 1B), and pathogenicity results (Fig. 1C) are presented in Fig. 1. Naturally infected nutmeg fruits exhibited typical black rot symptoms characterized by dense dark fungal mycelia on the fruit surface (Fig. 1A–a). Infected fruits showed tissue softening and dark brown to black discoloration of both pericarp and pulp, while cross-sections revealed desiccated tissues with extensive mycelial colonization (Fig. 1A and b).

Isolate NM-01 exhibited variable colony morphology depending on incubation conditions. On PDA at 28 ± 2 °C, colonies were initially dense, woolly, and creamy-white, later turning darker with concentric rings after 10 days (Fig. 1B, c–d). At 35 °C, colonies showed pinkish pigmentation at the margins (Fig. 1B–e–f). After 30 days at 28 ± 2 °C, dark colonies with pycnidia formation were observed (Fig. 1B–g). Mycelia were dark brown and septate, and conidia were ovoid to ellipsoidal, with sizes ranging from 44.2 to 56.6 μm × 21.6–29.5 μm (n = 30) (Fig. 1B–h–i).

Pathogenicity tests confirmed Koch's postulates. Inoculated nutmeg fruits developed black necrotic lesions within 5 days, accompanied by internal tissue discoloration and desiccation (Fig. 1C–j). Dense mycelial growth in cross-sections closely resembled that observed in naturally infected fruits (Fig. 1C–k).

3.2. Molecular identification of NM-01 pathogen

The molecular identification of the pathogen NM-01 is shown in Fig. 2. The ITS sequence showed a 100% match with *Lasiodiplodia theobromae* (PP768762.1); however, it did not effectively distinguish *L. theobromae* from its closely related species *L. brasiliensis* (OM102511.1) (Fig. 2A). In contrast, the LSU sequence exhibited 100% similarity to *L. theobromae* (KC442316.1, MN181372.1, and ON954596.1) (Fig. 2B). Therefore, based on the combined morphological characteristics and molecular analyses, isolate NM-01 was conclusively identified as *L. theobromae*.

3.3. Antagonist isolation and screening against L. theobromae in vitro

A total of 25 bacterial isolates were obtained from chili rhizosphere soil and screened for antagonistic activity against *L. theobromae* using a two-step process (Table 1). In the first step, all isolates were evaluated using the dual culture assay. Significant differences ($p < 0.05$) in mycelial growth and percentage inhibition were observed among the isolates. All bacterial strains suppressed the fungal pathogen to varying degrees, with inhibition ranging from 4.76% to 81.91%. Five isolates showed more than 50% inhibition, and the highest inhibition was recorded for C-KT-3 (81.91%).

In the second step, isolates exhibiting more than 40% inhibition in the dual culture assay were further tested for the production of VOCs using the sealed plate technique. The VOC assay showed that only a few isolates produced VOCs capable of inhibiting *L. theobromae*, with inhibition levels generally low, reaching a maximum of 27.95% (Table 1). Therefore, isolates exhibiting VOC-mediated inhibition were not selected for further evaluation. These findings indicate that while several isolates effectively inhibited the pathogen through direct contact, VOC-mediated inhibition was weak in most cases. C-KT-3, which showed the strongest antifungal activity in non-volatile assays, was selected as the most promising candidate for subsequent biocontrol studies.

3.4. Whole-genome sequencing, taxonomic identification, and analysis of secondary metabolite biosynthetic gene clusters in C-KT-3

Whole-genome sequencing of C-KT-3 was carried out using the Illumina platform, followed by *de novo* assembly with Unicycler, as detailed in Table 2. The assembly produced a single circular chromosome with a genome size of 5,401,338 bp and a GC content of 37.75%, consistent with a high-quality genome assembly. Genome visualization using the circlize package revealed a well-defined chromosomal organization with evenly distributed genomic features. Genome annotation predicted 5478 protein-coding sequences (CDSs), together with 58 tRNA genes and four rRNA genes. A circular genome map of C-KT-3 is shown in Fig. 3.

Phylogenomic analysis based on concatenated core-gene sequences was conducted using AutoMLST2 to resolve the taxonomic affiliation of C-KT-3. The analysis positioned C-KT-3 within the *Priestia aryabhattai* clade, where it clustered with the reference genome *P. aryabhattai* GCF_000956595 in a well-supported monophyletic group. The maximum-likelihood phylogenomic tree generated by AutoMLST2 and visualized using FigTree v1.4.4 displayed a stable topology with high bootstrap support across major nodes (Fig. 4). These findings support the assignment of C-KT-3 to the species *Priestia aryabhattai*.

Genome mining analysis of *P. aryabhattai* C-KT-3 using antiSMASH v6.0.1 revealed a diverse repertoire of BGCs associated with secondary metabolite production (Table 3). A total of ten putative BGCs were identified, representing multiple biosynthetic classes, including terpenes, ribosomally synthesized and post-translationally modified peptides (RiPPs), siderophores, polyketides, and beta-lactones. Among these, eight BGCs exhibited high similarity to previously characterized clusters deposited in the MIBiG database. Notably, terpene-associated gene clusters were predominant and showed high similarity to clusters involved in the biosynthesis of fumihopaside A, biarylitide YYH, sodorifen, and carotenoids. In addition, two lassopeptide clusters displayed high similarity to paeninodin and lariatin biosynthetic gene clusters, respectively. A nonribosomal-independent siderophore (NI-siderophore) cluster related to schizokinen biosynthesis was also identified with high similarity. In contrast, two BGCs showed low similarity to known MIBiG entries, including a beta-lactone cluster related to 1-heptadecene and a type III polyketide synthase (T3PKS) cluster associated with benzoquinone-related compounds. The presence of these low-similarity clusters suggests potential genetic divergence from previously described biosynthetic pathways.

3.5. Assessment of antifungal activity of P. aryabhattai C-KT-3 culture filtrates against L. theobromae

The antifungal activity of C-KT-3 CFs at concentrations ranging from 1% to 60% (v/v) was evaluated using both PDA and PDB media, and the results are summarized in Table 4. Significant differences ($p < 0.05$) in the growth of *L. theobromae* were observed among the different concentrations of CFs in both media. In PDA, the radial growth of the fungal pathogen in the control reached 9.00 cm, which was reduced to 4.15 cm at 60% (v/v) CFs, corresponding to 53.89% inhibition (Table 4A). Co-incubation of *L. theobromae* with C-KT-3 CFs resulted in a marked reduction in fungal biomass compared to the control in the solid co-cultivation assay, indicating a strong antagonistic effect of the bacterial bioagent.

Similarly, in PDB medium, increasing concentrations of CFs progressively reduced the mycelial dry weight from 153.57 mg in the control to 0.57 mg at 60% (v/v) (Table 4B). At 30% (v/v), CFs inhibited fungal growth by more than 53%, exceeding the inhibition observed on PDA (31.67%). At 60% (v/v), CFs almost completely suppressed pathogen growth in PDB (99.63%), whereas only 53.89% inhibition was observed on PDA. These findings indicate that CFs exhibited greater antifungal effects under liquid culture conditions than on solid medium. Overall, the results suggest that the antifungal activity of C-KT-3 CFs

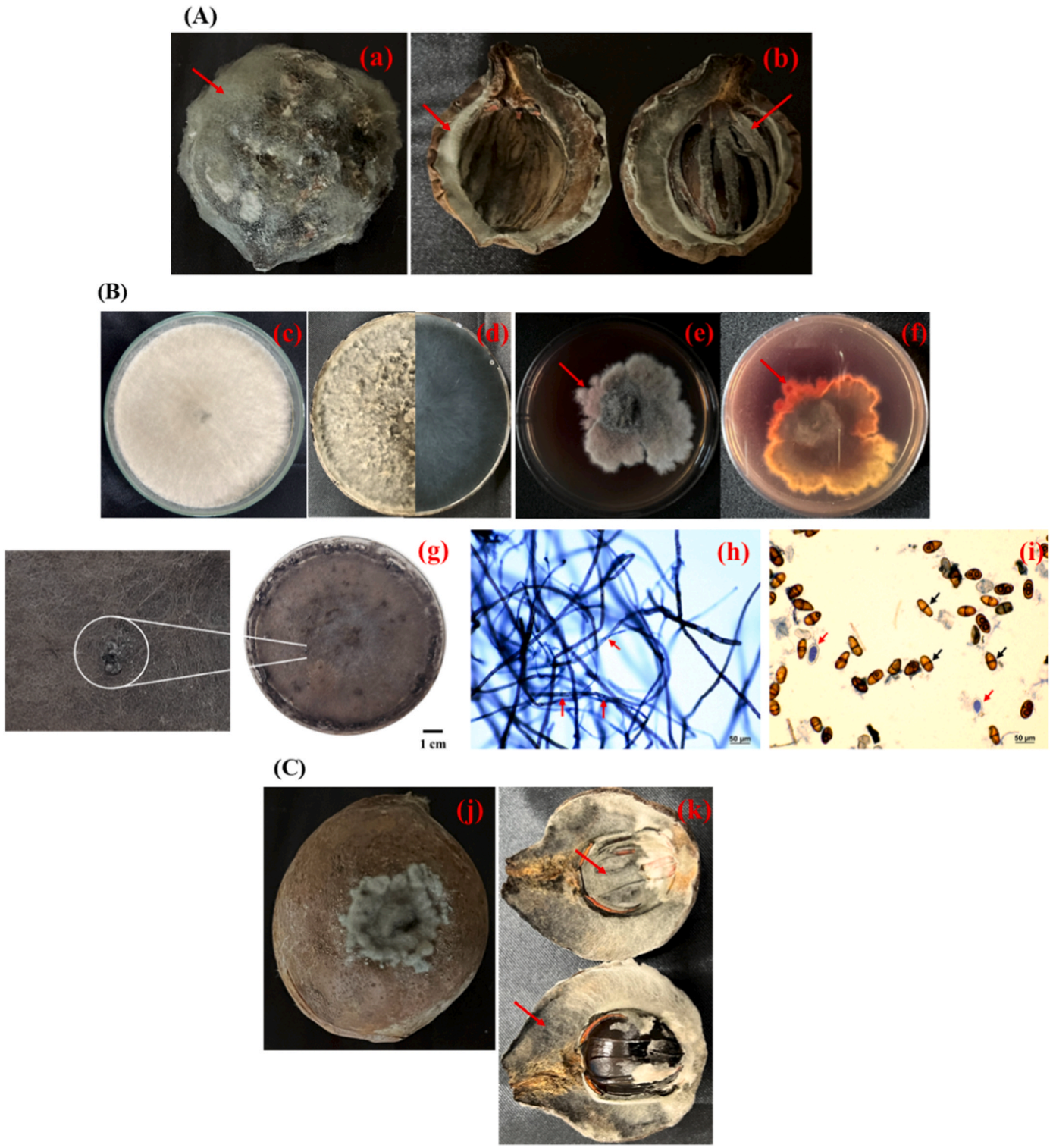

Fig. 1. Field symptoms, micromorphological characteristics, and pathogenicity of *L. theobromae* NM-01 causing nutmeg black rot.
(A) Disease symptoms of field-infected nutmeg fruits: **(a)** external symptoms showing necrotic lesions and extensive fungal mycelial growth on the fruit surface; **(b)** cross-section showing internal discoloration and tissue decay with dense mycelial colonization.
(B) Colony and micromorphological characteristics of NM-01 on PDA: **(c–d)** colony development at 28 ± 2 °C showing initial creamy, cottony mycelium and later concentric ring formation; **(e–f)** colony morphology at 35 °C showing pinkish pigmentation at the colony margin; **(g)** mature colony with pycnidia formation after 30 days at 28 ± 2 °C; **(h)** septate mycelium; **(i)** young and mature conidia.
(C) Pathogenicity test on nutmeg fruit: **(j)** external symptoms on inoculated fruit; **(k)** internal tissue decay confirming Koch's postulates.

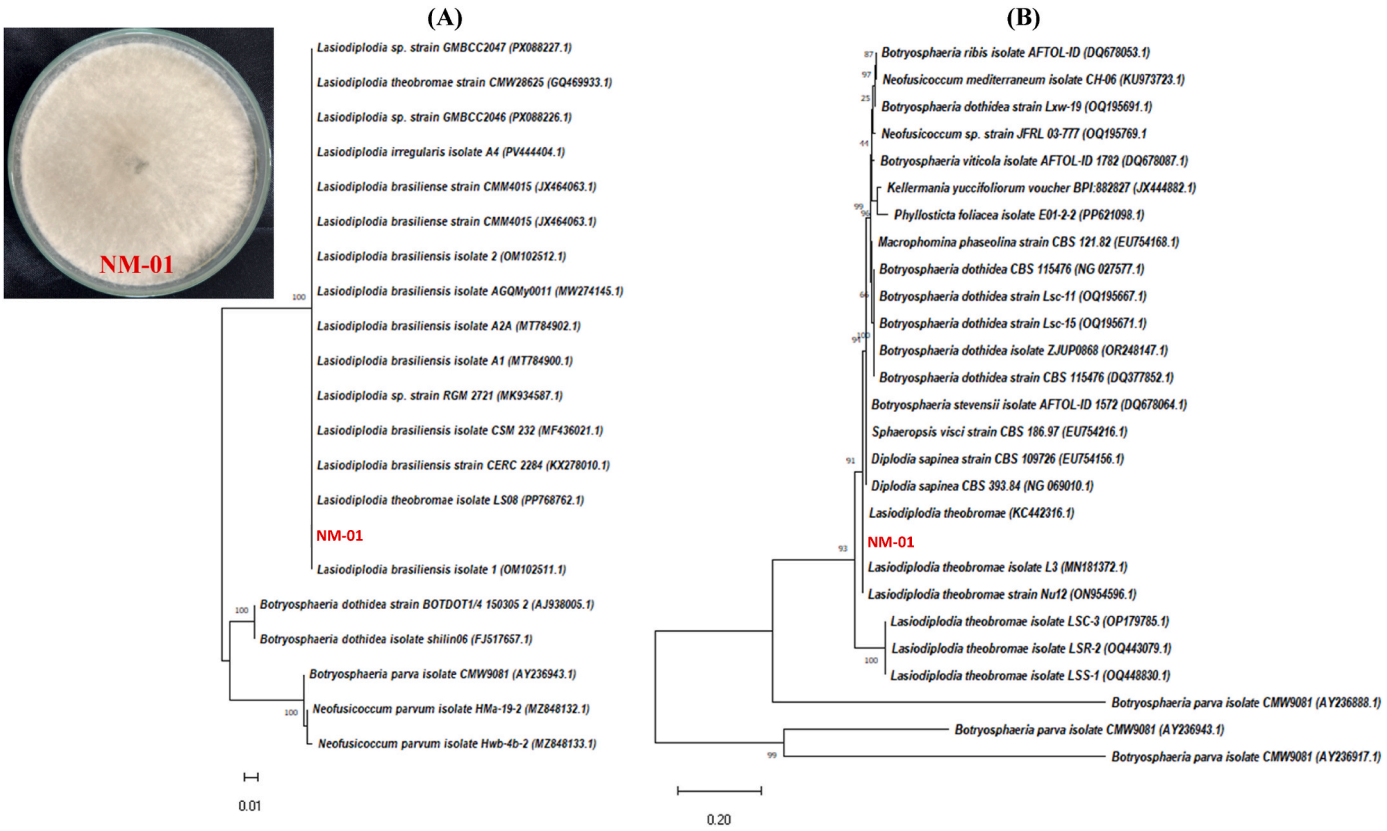

Fig. 2. Molecular identification of *L. theobromae* NM-01 isolated from symptomatic nutmeg fruit. Phylogenetic trees were constructed using the maximum-likelihood method based on sequences of the **(A)** internal transcribed spacer (ITS) region and **(B)** large subunit (LSU; 26S rRNA) gene. These sequences were compared with those of related *Lasiodiplodia* spp. type strains. The scale bars represent 0.01 and 0.02 substitutions per site for the ITS and LSU trees, respectively. Bootstrap support values were calculated based on 1000 replicates. NM-01, identified as *L. theobromae*, is highlighted in bold red. The phylogenetic trees were midpoint-rooted. (For interpretation of the references to color in this figure legend, the reader is referred to the Web version of this article.)

varies between liquid (PDB) and solid (PDA) assay systems, highlighting the influence of experimental conditions on the evaluation of antifungal potential.

3.6. Comparative efficacy of *P. aryabhattai* C-KT-3 culture filtrates with commercial fungicides and preservatives against *L. theobromae*

C-KT-3 CFs significantly inhibited ($p < 0.05$) the growth of *L. theobromae* compared to the control, with notable differences observed among the five commercial fungicides tested at concentrations of 0.1–0.8% (v/v) (Table 5). At 60% (v/v), the CFs reduced fungal radial growth by 53.89%, which exceeded the maximum inhibition achieved by azoxystrobin (35.56% at 0.8%). Prochloraz and propiconazole were the most effective, completely suppressing fungal growth (100%) at concentrations ≥0.2% (v/v), whereas thiram and metalaxyl achieved 89.44% and 88.52% inhibition, respectively, at 0.8%. These results indicate that C-KT-3 CFs could serve as a biological alternative to less effective fungicides such as azoxystrobin or be integrated into disease management strategies to reduce chemical use.

Regarding preservatives, C-KT-3 CFs exhibited antifungal activity (53.89%) comparable to sodium propionate at 0.10% (w/v) (53.89%), but slightly lower than sodium benzoate at 0.20% (w/v), which showed the highest inhibition (71.11%) (Table 6). These findings suggest that C-KT-3 CFs have potential as a natural alternative to synthetic preservatives for controlling *L. theobromae*, particularly in applications where minimizing chemical preservatives is desirable.

3.7. Broad-spectrum antifungal activity of *P. aryabhattai* C-KT-3 culture filtrates against plant pathogenic fungi

The broad-spectrum antifungal activity of C-KT-3 CFs against ten plant pathogenic fungi is presented in Fig. 5. The CFs significantly ($p < 0.05$) inhibited the mycelial growth of *R. solani*, *S. rolfsii*, *C. oryzae*, *A. flavus*, *A. parasiticus*, *S. commune*, *C. musae*, *C. cassiicola*, *F. incarnatum*, and *P. salaccae* (Fig. 5A–C), with inhibition levels ranging from 47.78% to 99.90% (Fig. 5B). Among these pathogens, *R. solani* (99.90%), *S. rolfsii* (99.43%), and *C. musae* (96.96%) were almost completely inhibited, indicating a strong antifungal effect. In contrast, *A. flavus* (50.76%), *F. incarnatum* (49.35%), and *P. salaccae* (47.78%) showed comparatively lower sensitivity to the CFs. Overall, these results suggest that C-KT-3 produces metabolites with broad-spectrum antifungal activity, highlighting its potential as a promising biocontrol agent for plant disease management.

3.8. LC–QTOF–MS-based identification of antifungal metabolites in culture filtrates of *P. aryabhattai* C-KT-3

LC–QTOF–MS analysis of the culture filtrates of *P. aryabhattai* C-KT-3 detected 54 compounds in the negative ion mode (−ESI) and 39 compounds in the positive ion mode (+ESI) (Tables S1 and S2, Supplementary data). All metabolites were putatively identified based on LC–QTOF–MS spectral database matching. It should be noted that these identifications are tentative and based on database matching, and therefore may include isobaric or false-positive annotations; structural confirmation is required for validation.

The −ESI mode mainly detected amino acids, short peptides, organic

Table 1
Inhibition percentages of bacterial isolates against *L. theobromae* mycelial growth on NA plates using dual culture and sealed plate assays after 3 days of incubation at 28 ± 2 °C.

Treatment	Dual culture assay		Sealed plate assay	
	Radial growth (cm)	Inhibition (%)	Radial growth (cm)	Inhibition (%)
Control	$4.70^{a} \pm 0.85$	-	$8.77^{bc} \pm 0.33$	-
C-KT-2	$3.65^{de} \pm 0.46$	$16.57^{k} \pm 1.16$	-	-
C-KT-3	$0.85^{l} \pm 0.08$	$81.91^{a} \pm 1.51$	$9.00^{a} \pm 0.00$	−2.66
C-KT-5	$4.17^{b} \pm 0.51$	$4.76^{l} \pm 0.59$	-	-
C-KT-6	$2.06^{jk} \pm 0.55$	$56.21^{c} \pm 1.33$	$8.90^{ab} \pm 0.22$	−1.52
C-KT-7	$3.78^{bcde} \pm 0.33$	$13.52^{k} \pm 2.58$	-	-
C-KT-8	$4.19^{b} \pm 1.24$	$4.19^{l} \pm 0.80$	-	-
C-KT-10	$2.37^{ij} \pm 0.77$	$49.65^{de} \pm 0.75$	$8.82^{bc} \pm 0.41$	−0.57
C-KT-11	$2.66^{hi} \pm 0.28$	$39.24^{fg} \pm 0.60$	$8.67^{c} \pm 0.55$	1.14
C-KT-12	$2.83^{gh} \pm 0.42$	$35.24^{gh} \pm 2.01$	-	-
C-KT-13	$3.99^{bcd} \pm 0.51$	$15.07^{k} \pm 1.53$	-	-
C-KT-14	$3.65^{de} \pm 0.52$	$16.57^{k} \pm 1.05$	-	-
C-KT-15	$1.70^{k} \pm 0.06$	$63.83^{b} \pm 0.85$	$6.32^{f} \pm 3.13$	27.95
C-KT-17	$3.93^{bcd} \pm 0.19$	$16.49^{k} \pm 0.83$	-	-
C-KT-18	$3.61^{de} \pm 0.31$	$23.23^{j} \pm 1.84$	-	-
C-KT-19	$2.22^{j} \pm 0.70$	$52.84^{cd} \pm 0.89$	$9.00^{a} \pm 0.00$	−2.66
C-KT-20	$3.57^{de} \pm 0.38$	$24.14^{j} \pm 1.95$	-	-
C-KT-22	$3.11^{fg} \pm 0.34$	$40.51^{f} \pm 2.93$	$8.32^{d} \pm 0.62$	5.13
C-KT-23	$3.73^{cde} \pm 0.46$	$28.71^{i} \pm 1.07$	-	-
C-KT-26	$2.64^{hi} \pm 0.29$	$49.44^{de} \pm 1.93$	$9.00^{a} \pm 0.00$	−2.66
C-KT-29	$3.56^{de} \pm 0.45$	$31.90^{hi} \pm 0.77$	-	-
C-KT-30	$2.80^{gh} \pm 0.42$	$46.41^{e} \pm 0.85$	$7.53^{e} \pm 1.15$	16.30
C-KT-31	$4.20^{b} \pm 0.12$	$4.00^{l} \pm 1.22$	-	-
C-KT-33	$3.41^{ef} \pm 0.43$	$34.77^{gh} \pm 1.74$	-	-
C-KT-34	$4.08^{bc} \pm 0.80$	$22.01^{j} \pm 0.65$	-	-
C-KT-35	$2.28^{ij} \pm 0.71$	$56.46^{c} \pm 1.14$	$8.73^{bc} \pm 0.39$	0.38

Note: Data are expressed as the mean ± SD (n = 3). Means followed by different letters are significantly different according to Tukey's HSD test (ANOVA, $p < 0.05$).

Table 2
Genome features of *P. aryabhattai* C-KT-3.

Feature	Chromosome characteristics
Genome size(bp)	5401338
GC Content (%)	37.75
CDS No.	5478
tRNA No.	58
rRNA No.	4
Gene Average Len (bp)	816
Secondary metabolite gene clusters	10

acids, and nucleotide-related metabolites, including lysine, valine, citric acid, succinic acid, inosine, and xanthine. In contrast, the +ESI mode mainly revealed nitrogen-containing metabolites, including amino acid derivatives, short peptides, and other peptide-based structures. Comparison of both ionization modes indicated complementary metabolite coverage, where −ESI favored polar acidic compounds, while + ESI preferentially detected protonated nitrogen-containing and peptide-related metabolites.

3.9. Evaluation of P. aryabhattai C-KT-3 efficacy in controlling nutmeg black rot and maintaining fruit quality

3.9.1. Evaluation of C-KT-3 efficacy in controlling nutmeg black rot

The biocontrol ability of C-KT-3 CFs (CFs; 25, 50, 75, and 100% v/v) and bacterial cell suspensions (10^5, 10^6, 10^7, and 10^8 CFU/mL) against *L. theobromae* is illustrated in Figs. 6 and 7, respectively. Application of CFs significantly ($p < 0.05$) reduced lesion development on nutmeg fruits compared with the positive control (fruits inoculated with

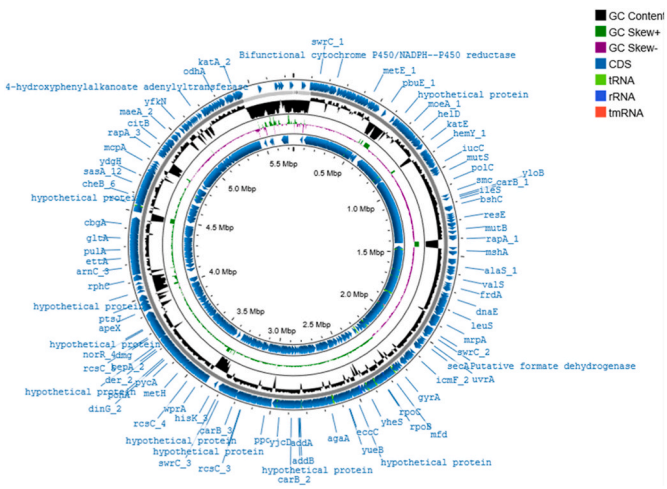

Fig. 3. Circular representation of *P. aryabhattai* C-KT-3 genome for several specific genome features.

L. theobromae but without CFs treatment) and the negative control/untreated fruits (non-inoculated, no treatment), with lesion diameter decreasing progressively as CFs concentration increased (Fig. 6A–C). The strongest suppression was observed at 100% CFs, which reduced the lesion size from 3.22 cm^2 in the positive control to 0.70 cm^2, achieving the highest disease control of 78.26% (Fig. 6B), indicating that full-strength CFs exerted the most effective antifungal activity.

Similarly, treatment with bacterial cell suspensions also resulted in a significant ($p < 0.05$) decrease in lesion development compared with the positive and negative controls (Fig. 7). The highest efficacy was recorded at 10^8 CFU/mL, which reduced the lesion diameter to 0.77 cm^2 and provided 76.0% disease control (Fig. 7A–C). These results demonstrate a clear concentration-dependent response, with higher cell densities providing greater biocontrol activity. Overall, both the CFs and bacterial cells of C-KT-3 showed strong and concentration-dependent biocontrol potential, suggesting that both active extracellular metabolites and viable cells contribute to the effective suppression of *L. theobromae* on nutmeg fruits.

3.9.2. Evaluation of the effects of NM-01 inoculation and C-KT-3 treatment on nutmeg fruit quality

Both cell suspension (Fig. 8A–a–d) and culture filtrates (Fig. 8B–e–h) treatments of C-KT-3 significantly influenced postharvest quality attributes of nutmeg fruits, although distinct response patterns were observed between the two treatment types (Fig. 8). For cell suspension treatments (Fig. 8A), total soluble solids were maintained at levels comparable to the negative control only at the highest concentration (10^8 CFU/mL), whereas significantly lower values were observed at lower concentrations. Titratable acidity increased progressively with increasing cell concentration, reaching the highest level at 10^8 CFU/mL. Total phenolic content and antioxidant capacity were better preserved at 10^7–10^8 CFU/mL, with maximum antioxidant activity observed at 10^7 CFU/mL (Fig. 8A).

In contrast, culture filtrates treatments (Fig. 8B) showed a clear concentration-dependent response. Total soluble solids were lowest in the positive control, while all filtrate treatments resulted in higher values than the positive control, although still below the negative control. Titratable acidity increased with increasing filtrate concentration, reaching peak levels at 75% and 100%. Total phenolic content increased in a concentration-dependent manner, with the highest retention observed at 100%, followed by 75% and 50%. Consistently, antioxidant activity was significantly enhanced at higher filtrate concentrations, with 75% and 100% treatments showing the highest activity.

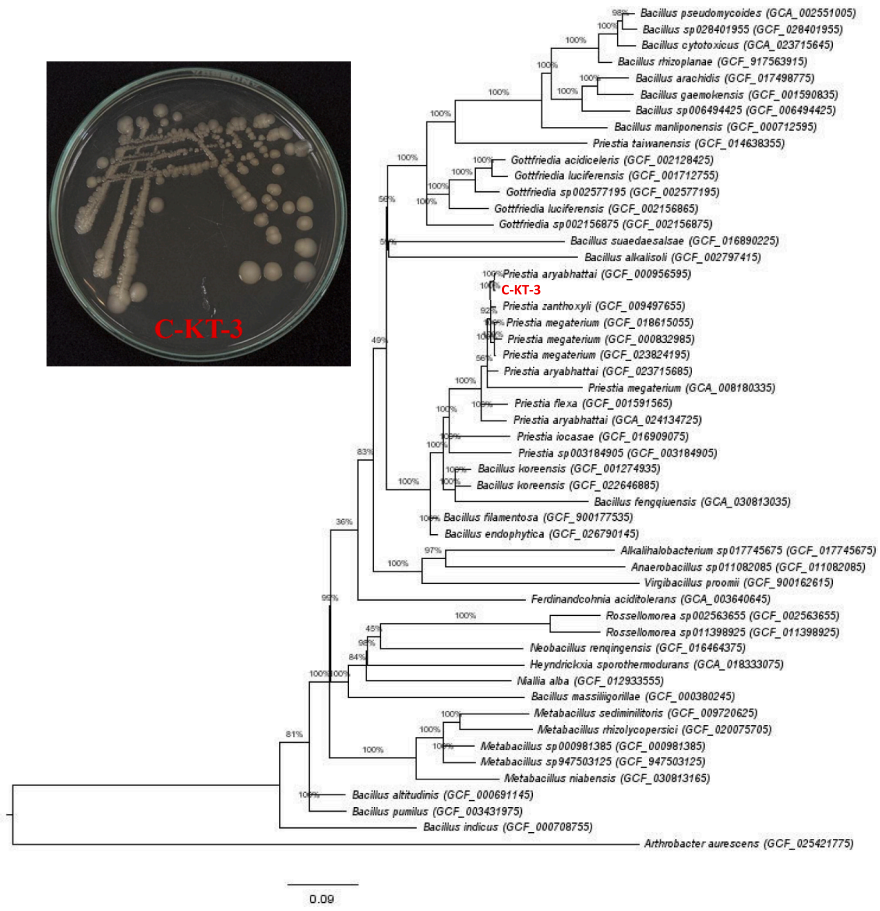

Fig. 4. Maximum-likelihood phylogenomic tree inferred from concatenated core genes using AutoMLST2 with IQ-TREE. The scale bar represents 0.09 substitutions per site. Bootstrap support values were calculated based on 1000 replicates. C-KT-3, identified as *Priestia aryabhattai*, is highlighted in bold red. The phylogenetic trees were midpoint-rooted. (For interpretation of the references to color in this figure legend, the reader is referred to the Web version of this article.)

Table 3
Prediction of biosynthetic gene clusters (BGCs) of secondary metabolites in *P. aryabhattai* C-KT-3 using antiSMASH V6.0.1.

Region	Type	Start	End	MIBIG accession	Most similar known cluster	Similarity confidence
Region 1.1	terpene	381,623	403,491	BGC0002173.2	fumihopaside A	High
Region 1.2	lassopeptide	434,917	463,703	BGC0001356.4	paeninodin	High
Region 1.3	terpene	2,002,407	2,023,225	BGC0002084.4	biarylitide YYH	High
Region 1.4	NI-siderophore	2,184,288	2,218,860	BGC0002683.2	schizokinen	High
Region 1.5	terpene-precursor	2,591,326	2,612,222	BGC0002283.2	sodorifen	High
Region 2.1	betalactone	1	26,155	BGC0001164.3	1-heptadecene	Low
Region 2.2	T3PKS	301,281	342,366	BGC0000282.3	2-methoxy-5-methyl-6-(13-methyltetradecyl)-1,4-benzoquinone, 2-methoxy-5-methyl-6-(13-methyltetradecyl) phenol	Low
Region 2.3	terpene	1,108,251	1,129,099	BGC0000647.3	carotenoid	High
Region 4.1	lassopeptide	26,832	49,290	BGC0000575.5	lariatin	High
Region 14.1	ranthipeptide	2368	23,729	BGC0000851.5	albonoursin	High

3.10. Mycolytic activity and antifungal mechanisms of P. aryabhattai C-KT-3

3.10.1. Mycolytic activity

The mycolytic activity of *P. aryabhattai* C-KT-3 against *L. theobromae* is shown in Fig. 9. The mycolytic potential of C-KT-3 was evaluated in a nutrient-poor medium (1000× diluted nutrient broth) co-cultured with *L. theobromae* to assess its ability to utilize fungal biomass as a nutrient source. Following incubation, bacterial population analysis revealed that the presence of fungal biomass markedly promoted bacterial

Table 4
Effect of *P. aryabhattai* C-KT-3 culture filtrates (CFs) concentration (1–60% v/v) on the growth of *L. theobromae* on PDA **(A)** and in PDB **(B)** after 3 days of incubation at 28 ± 2 °C.

(A)						
Parameter	Concentration of C-KT-3 CFs (% v/v)					
	Control	1	15	30	45	60
Radial growth (cm)	$9.00^{a} \pm 0.00$	$8.65^{a} \pm 0.45$	$7.70^{ab} \pm 0.10$	$6.15^{bc} \pm 1.40$	$5.38^{bc} \pm 0.72$	$4.15^{c} \pm 0.54$
Inhibition (%)	-	$3.89^{e} \pm 0.39$	$14.44^{d} \pm 0.41$	$31.67^{c} \pm 2.09$	$40.19^{b} \pm 1.30$	$53.89^{a} \pm 0.54$
Colony morphology	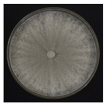	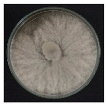	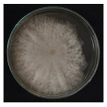	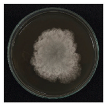	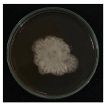	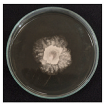
(B)						
Mycelial dry weight (mg/10 mL)	$153.57^{a} \pm 6.91$	$131.17^{ab} \pm 0.73$	$117.23^{ab} \pm 1.70$	$72.167^{bc} \pm 2.76$	$2.93^{c} \pm 0.81$	$0.57^{c} \pm 0.08$
Inhibition (%)	-	$14.59^{e} \pm 0.68$	$23.66^{d} \pm 1.76$	$53.01^{c} \pm 0.62$	$87.24^{b} \pm 0.69$	$99.63^{a} \pm 0.32$
Colony morphology		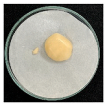	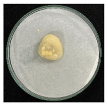			

Note: Data are expressed as the mean ± SD (n = 3). Means followed by different letters are significantly different according to Tukey's HSD test (ANOVA, $p < 0.05$).

Table 5
Comparative efficacy of *P. aryabhattai* C-KT-3 culture filtrates (CFs) and commercial fungicides against *L. theobromae* on PDA medium after incubation at 28 ± 2 °C for 3 days.

Treatment	Concentration (% v/v)	Radial growth (cm)	Inhibition (%)
Control		$9.00^{a} \pm 0.00$	-
C-KT-3 CFs	60	$4.15^{e} \pm 0.54$	$53.89^{g} \pm 0.54$
Metalaxyl			
	0.1	$8.02^{ab} \pm 0.03$	$10.93^{k} \pm 0.32$
	0.2	$7.47^{bc} \pm 0.45$	$17.04^{jk} \pm 0.05$
	0.4	$3.02^{e} \pm 0.03$	$66.48^{f} \pm 0.32$
	0.6	$1.35^{fgh} \pm 0.20$	$85.00^{bc} \pm 0.22$
	0.8	$1.03^{ghi} \pm 0.08$	$88.52^{b} \pm 0.85$
Prochloraz			
	0.1	$1.55f^{gh} \pm 0.43$	$82.78^{bcd} \pm 4.81$
	0.2	$0.00^{i} \pm 0.00$	$100.00^{a} \pm 0.00$
	0.4	$0.00^{i} \pm 0.00$	$100.00^{a} \pm 0.00$
	0.6	$0.00^{i} \pm 0.00$	$100.00^{a} \pm 0.00$
	0.8	$0.00^{i} \pm 0.00$	$100.00^{a} \pm 0.00$
Azoxystrobin			
	0.1	$7.67^{bc} \pm 0.58$	$14.81^{jk} \pm 0.40$
	0.2	$7.27^{bc} \pm 0.55$	$19.26^{jk} \pm 0.10$
	0.4	$7.03^{bc} \pm 0.90$	$21.85^{ij} \pm 1.20$
	0.6	$6.48^{cd} \pm 0.43$	$27.96^{hi} \pm 0.71$
	0.8	$5.80^{d} \pm 0.44$	$35.56^{h} \pm 0.94$
Propiconazole			
	0.1	$0.92^{hi} \pm 0.08$	$89.81^{b} \pm 0.85$
	0.2	$0.00^{i} \pm 0.00$	$100.00^{a} \pm 0.00$
	0.4	$0.00^{i} \pm 0.00$	$100.00^{a} \pm 0.00$
	0.6	$0.00^{i} \pm 0.00$	$100.00^{a} \pm 0.00$
	0.8	$0.00^{i} \pm 0.00$	$100.00^{a} \pm 0.00$
Thiram			
	0.1	$2.50^{ef} \pm 0.05$	$72.22^{ef} \pm 0.56$
	0.2	$2.23^{efg} \pm 0.23$	$75.19^{de} \pm 2.47$
	0.4	$2.13^{efgh} \pm 0.13$	$76.30^{cde} \pm 1.40$
	0.6	$1.55^{fgh} \pm 0.09$	$82.78^{bcd} \pm 0.96$
	0.8	$0.95^{hi} \pm 0.00$	$89.44^{b} \pm 0.52$

Note: Data are expressed as the mean ± SD (n = 3). Means followed by different letters are significantly different according to Tukey's HSD test (ANOVA, $p < 0.05$).

proliferation. The population of C-KT-3 reached 5.87 log CFU/mL in co-culture with *L. theobromae*, whereas the control without fungal biomass showed a substantially lower population of 3.85 log CFU/mL, representing an increase of approximately 2 log units. Both the spotting assay (Fig. 9A) and CFU enumeration (Fig. 9B) consistently demonstrated that C-KT-3 was capable of degrading and utilizing fungal biomass for growth under nutrient-limited conditions.

Table 6
Comparative efficacy of *P. aryabhattai* C-KT-3 culture filtrates (CFs) and commercial preservatives against *L. theobromae* on PDA medium after incubation at 28 ± 2 °C for 3 days.

Treatment	Concentration (% v/v or w/v)	Radial growth (cm)	Inhibition (%)
Control		$9.00^{a} \pm 0.00$	-
C-KT-3 CFs	60	$4.15^{bc} \pm 0.54$	$53.89^{e} \pm 0.54$
Sodium benzoate			
	0.05	$4.52^{b} \pm 0.47$	$49.81^{f} \pm 0.47$
	0.10	$4.02^{cd} \pm 0.41$	$55.37^{e} \pm 0.41$
	0.15	$3.17^{e} \pm 0.14$	$64.81^{c} \pm 0.14$
	0.20	$2.60^{f} \pm 0.28$	$71.11^{a} \pm 0.28$
Sodium propionate			
	0.05	$4.18^{bc} \pm 0.21$	$53.52^{e} \pm 0.21$
	0.10	$4.15^{bc} \pm 0.21$	$53.89^{e} \pm 0.21$
	0.15	$3.72^{d} \pm 0.34$	$58.70^{d} \pm 0.34$
	0.20	$2.92^{ef} \pm 0.16$	$67.59^{b} \pm 0.16$

Note: Data are expressed as the mean ± SD (n = 3). Means followed by different letters are significantly different according to Tukey's HSD test (ANOVA, $p < 0.05$).

3.10.2. *Oxidative stress–related mechanism*

The oxidative stress–related mechanism of action of *P. aryabhattai* C-KT-3 against *L. theobromae* is shown in Fig. 9. Treatment of *L. theobromae* with the CFs of *P. aryabhattai* C-KT-3 resulted in pronounced alterations in oxidative stress–related responses compared with the control (Fig. 9C–H). ROS levels increased from 171.23 to 241.40 μM/mg protein, representing an approximately 1.4-fold increase following CFs treatment (Fig. 9C). In parallel, SOD activity increased markedly from 9.79 to 29.02 Unit/min/mg protein, corresponding to an almost three-fold increase, while CAT activity increased from 33.70 to 54.65 Unit/min/mg protein, equivalent to an approximately 1.6-fold increase relative to the control (Fig. 9D and E).

In addition, GSH content increased from 5.95 to 9.65 μM/mg protein (approximately 1.6-fold), whereas GSSG levels decreased from 2.08 to 0.82 μM/mg protein, corresponding to a reduction to approximately 40% of the control level (Fig. 9F and G). Consequently, the GSH/GSSG ratio increased from 3.54 in the control to 5.02 in CFs-treated samples, indicating an enhanced glutathione-dependent antioxidant capacity in response to the CFs of *P. aryabhattai* C-KT-3 (Fig. 9H). These results suggest that CFs treatment induced oxidative stress, accompanied by activation of antioxidant defense mechanisms in the fungal cells.

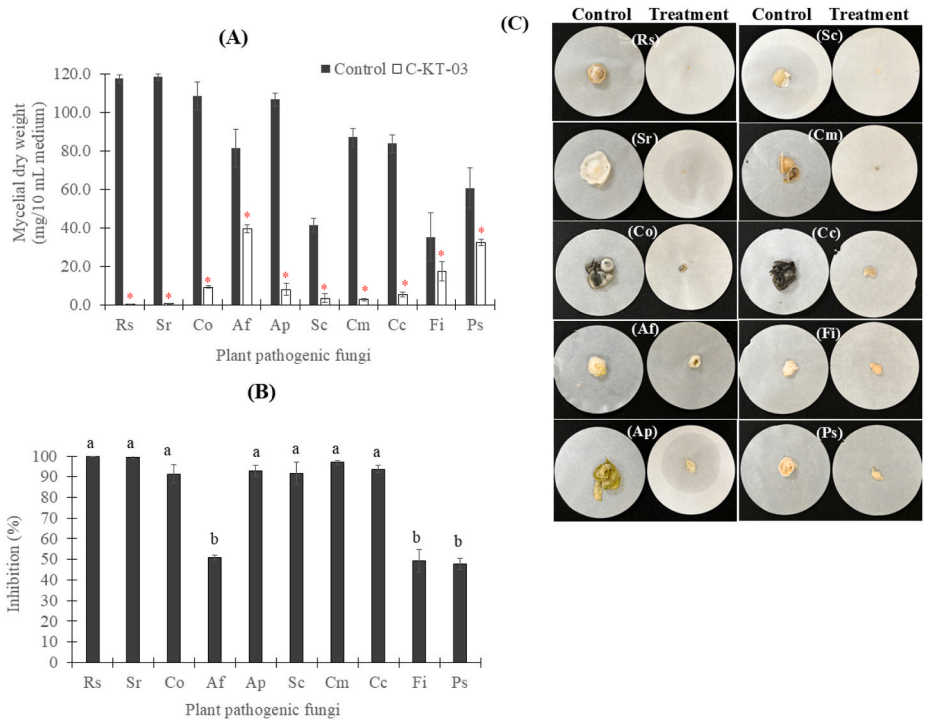

Fig. 5. Broad-spectrum antifungal activity of *P. aryabhattai* C-KT-3 culture filtrates (CFs) against ten plant pathogenic fungi.
(A) Mycelial growth inhibition of each fungal isolate treated with C-KT-3 CFs. Asterisks indicate significant differences between treated and control groups within each isolate (*$p < 0.05$). Data are expressed as the mean ± SD (n = 3).
(B) Percentage of growth inhibition among different fungal isolates. Means followed by different letters are significantly different ($p < 0.05$) according to Tukey's HSD test. Data are expressed as the mean ± SD (n = 3).
(C) Colony morphology of *R. solani* (Rs), *S. rolfsii* (Sr), *C. oryzae* (Co), *A. flavus* (Af), *A. parasiticus* (Ap), *S. commune* (Sc), *C. musae* (Cm), *C. cassiicola* (Cc), *F. incarnatum* (Fi), and *P. salaccae* (Ps) following exposure to C-KT-3 CFs, produced in PDB medium, incubated at 28 ± 2 °C for 3–7 days.

4. Discussion

Postharvest losses caused by fungal pathogens significantly affect fruit quality and yield worldwide. Antagonistic microorganisms, including *Bacillus*, *Streptomyces*, *Pseudomonas*, and *Priestia*, have been widely reported to suppress postharvest pathogens in several fruits such as strawberries, grapes, muskmelons, pear, and citrus (Cui et al., 2023; Lastochkina et al., 2019; Verma et al., 2022). However, information on biological control of postharvest nutmeg black rot remains limited. In this study, *L. theobromae* was confirmed as the causal agent of nutmeg black rot, consistent with its role in postharvest decay of other economically important fruits in Thailand and elsewhere (Che et al., 2015; Chen et al., 2021; Gariba et al., 2025; Kaewkrajay & Dethoup, 2024; Nur-Shakirah et al., 2022). These findings emphasize the urgent need for sustainable disease management strategies, particularly biocontrol approaches. The pathogen used in this study was isolated from a single orchard in southern Thailand; therefore, it may not fully represent the genetic and pathogenic diversity of *L. theobromae* populations in other nutmeg-growing regions. Accordingly, further studies involving multiple isolates from different geographic locations are required to validate and strengthen the general applicability of these findings.

Rhizosphere-associated bacteria are recognized as sustainable and effective antagonists of postharvest pathogens. Variability in inhibitory activity among isolates, commonly reported in microbial screening studies, was evident in this work. Among the tested isolates, C-KT-3 consistently exhibited the strongest contact-dependent suppression in dual culture assays, whereas VOC-mediated inhibition was weak. Interestingly, several isolates exhibited negative inhibition values in the VOCs assay, indicating a slight stimulation of fungal growth under sealed conditions. Such effects may arise from specific VOCs that can act as growth-promoting signals or serve as alternative carbon sources for the fungus. Previous studies have shown that microbial VOCs can exert dual effects—either inhibitory or stimulatory—in a concentration-dependent and compound-specific manner (Effmert et al., 2012; Kai et al., 2009). This pattern is consistent with previous reports in *Bacillus*- and *Priestia*-related systems, where inhibitory effects are mainly associated with direct microbial interactions and the production of diffusible antifungal metabolites, rather than volatile-mediated activity (Sajitha et al., 2016; Saucedo-Bazalar et al., 2023).

Although C-KT-15 exhibited the highest VOC-mediated inhibition among the tested isolates, VOC effects were generally low and inconsistent, with some strains even showing negative values. In contrast, strain C-KT-3 demonstrated the highest and most consistent inhibition in the dual culture assay, indicating that non-volatile mechanisms are the dominant mode of antagonism. Therefore, C-KT-3 was selected for further investigation based on its superior overall antifungal performance, suggesting that non-volatile diffusible compounds are the dominant mechanism of antagonism.

To place this antagonistic phenotype in a taxonomic and genomic context, strain C-KT-3 was assigned to *Priestia aryabhattai* based on whole-genome phylogenomic analyses. At the genomic level, this antagonistic behavior is further supported by genome mining, which provides mechanistic insight into the observed diffusion- and contact-mediated suppression of *L. theobromae* by *P. aryabhattai* C-KT-3. Similar genome-based studies on bacterial biocontrol agents have demonstrated that the presence of diverse BGCs is strongly associated with the production of antifungal secondary metabolites and enhanced ecological competitiveness (De la Cruz-Rodríguez et al., 2023; Zhou et al., 2021). The predominance of non-volatile BGCs identified in C-KT-3 further supports the hypothesis that antagonism is primarily mediated by diffusible metabolites rather than volatile compounds, a

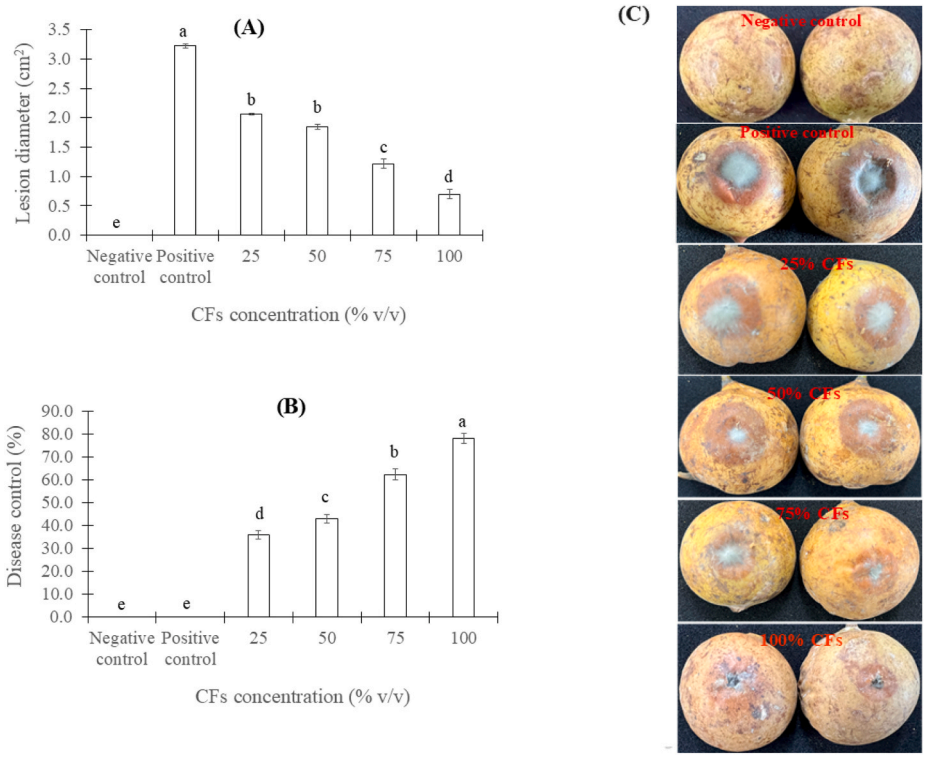

Fig. 6. Efficacy of *P. aryabhattai* C-KT-3 culture filtrates (CFs; 25, 50, 75, and 100% v/v) against nutmeg black rot. **(A)** Lesion diameter, **(B)** disease control, and **(C)** disease symptoms of nutmeg wounds inoculated with *L. theobromae*. The negative control consisted of non-inoculated and untreated fruits, whereas the positive control comprised fruits inoculated with the pathogen only. Means followed by different letters are significantly different ($p < 0.05$) according to Tukey's HSD test. Data are expressed as the mean ± SD (n = 18).

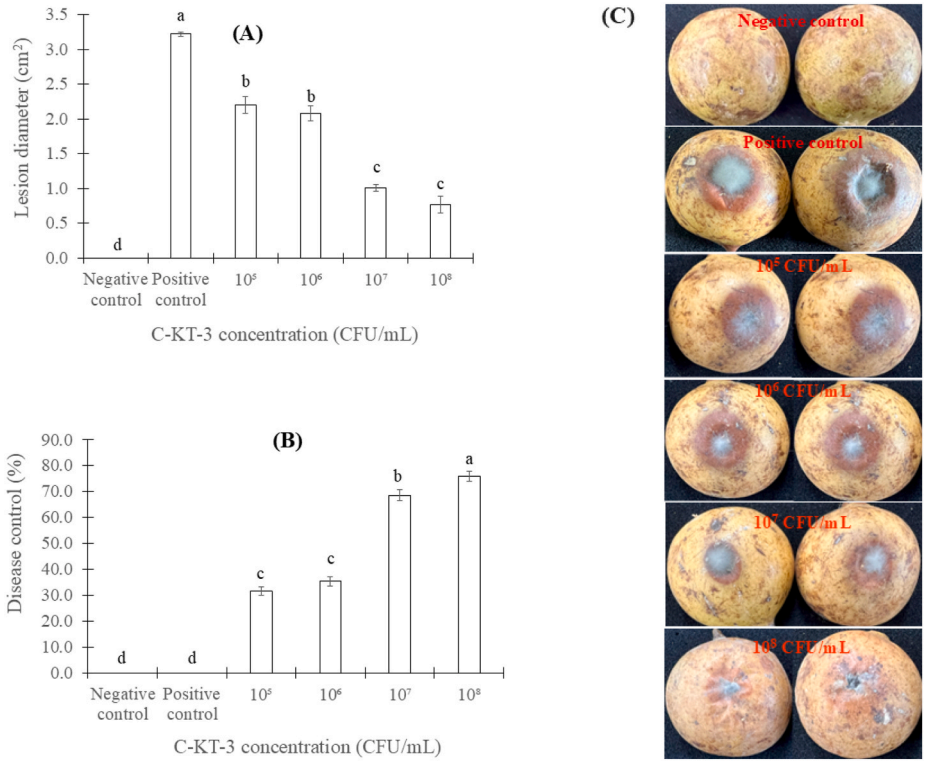

Fig. 7. Efficacy of *P. aryabhattai* C-KT-3 bacterial cell suspensions (10^5, 10^6, 10^7, and 10^8 CFU/mL) against nutmeg black rot. **(A)** Lesion diameter, **(B)** disease control, and **(C)** disease symptoms of nutmeg wounds inoculated with *L. theobromae*. The negative control consisted of non-inoculated and untreated fruits, whereas the positive control comprised fruits inoculated with the pathogen only. Means followed by different letters are significantly different ($p < 0.05$) according to Tukey's HSD test. Data are expressed as the mean ± SD (n = 18).

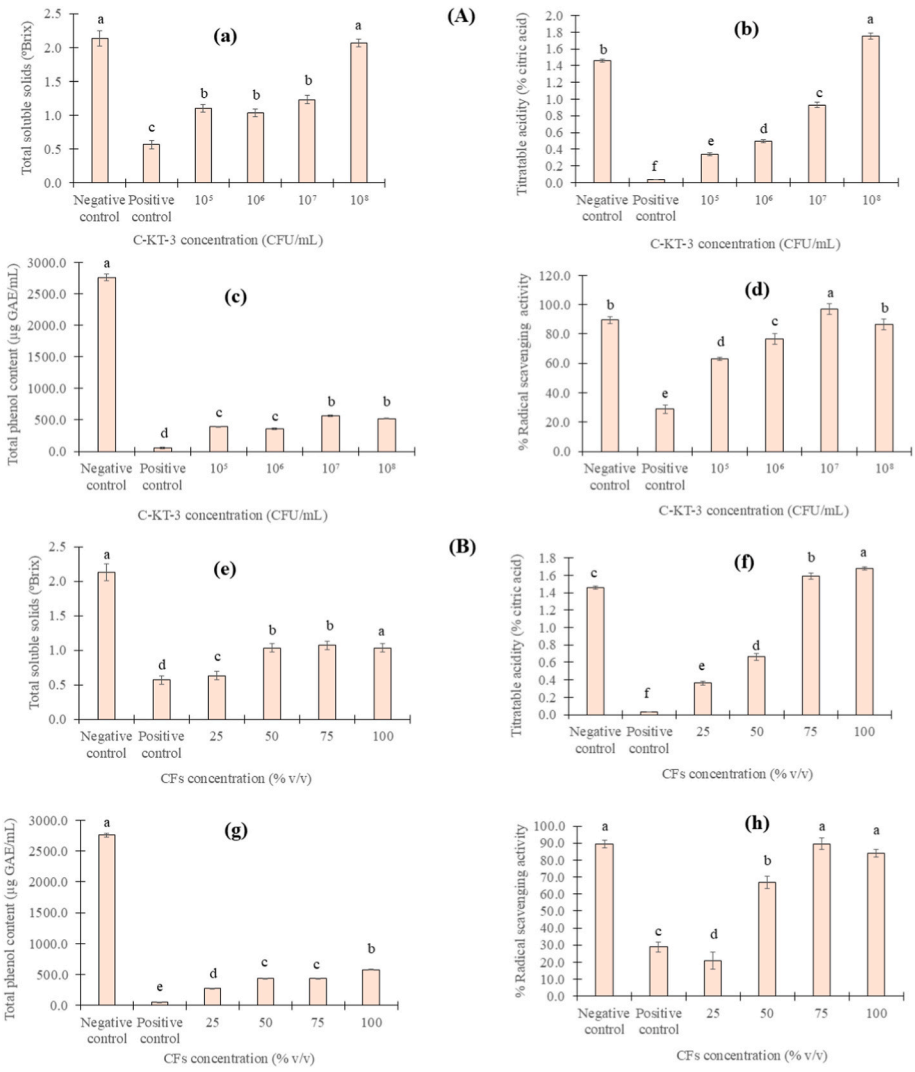

Fig. 8. Effects of *L. theobromae* infection and *P. aryabhattai* C-KT-3 treatments on postharvest quality of nutmeg fruits after 5 days of incubation at 30 °C under humid conditions.
(A) Cell suspension treatments: total soluble solids (°Brix) **(a)**, titratable acidity **(b)**, total phenolic content **(c)**, and radical scavenging activity **(d)**.
(B) Culture filtrates treatments: total soluble solids (°Brix) **(e)**, titratable acidity **(f)**, total phenolic content **(g)**, and radical scavenging activity **(h)**.
The negative control consisted of non-inoculated and untreated fruits, whereas the positive control comprised fruits inoculated with the pathogen only. Means followed by different letters are significantly different ($p < 0.05$) according to Tukey's HSD test. Data are expressed as the mean ± SD (n = 18).

mechanism widely reported in postharvest biocontrol systems (Carmona-Hernandez et al., 2019; Droby et al., 2009).

Terpene-associated gene clusters detected in *P. aryabhattai* C-KT-3 may contribute to fungal growth suppression through membrane destabilization and interference with cellular signaling pathways, mechanisms that have been widely reported for bacterial secondary metabolites produced by members of the *Bacillus* group (Caulier et al., 2019; Raaijmakers & Mazzola, 2012). In parallel, RiPP-related clusters, including lassopeptides, are known to encode structurally constrained and proteolytically stable antimicrobial peptides, which may contribute to their stability and sustained bioactivity under fluctuating environmental conditions typical of postharvest storage (Rowe & Spring, 2021). In addition to direct antifungal metabolites, the identification of a siderophore biosynthetic gene cluster suggests that iron sequestration may represent an additional antagonistic strategy employed by *P. aryabhattai* C-KT-3. Siderophore-mediated competition for iron has been recognized as a key mechanism by which bacterial antagonists suppress fungal pathogens on fruit surfaces and limit pathogen establishment during storage (Carmona-Hernandez et al., 2019; Fenta et al., 2023; Kumar et al., 2024).

The C-KT-3 CFs exhibited strong antifungal activity in both liquid (PDB) and solid (PDA) assays. Differences in inhibition levels observed between the two systems are likely attributable to variations in assay conditions, such as metabolite diffusion, medium composition, and interaction dynamics. Similar inconsistencies between liquid and solid assay systems have been reported in previous studies, where the activity of bacterial metabolites, including antibiotics, lipopeptides, and extracellular enzymes, is influenced by the physicochemical properties of the testing environment (de Fátima Dias Diniz et al., 2024; Prapagdee et al., 2008; Wang et al., 2022). Following the initial evaluation against selected chemical fungicides (e.g., azoxystrobin) and food preservatives (e.g., sodium propionate), the CFs were further tested against ten fungal species, demonstrating consistent broad-spectrum inhibitory activity. These findings highlight the potential of C-KT-3 CFs as biologically derived antifungal agents for postharvest disease management.

A relatively high concentration of culture filtrate (60% v/v) of *P. aryabhattai* C-KT-3 was required to achieve strong antifungal activity, resulting in 99.63% inhibition against *L. theobromae*. This level of efficacy falls within the upper range of those reported in previous studies using different antagonistic microorganisms. For instance, culture

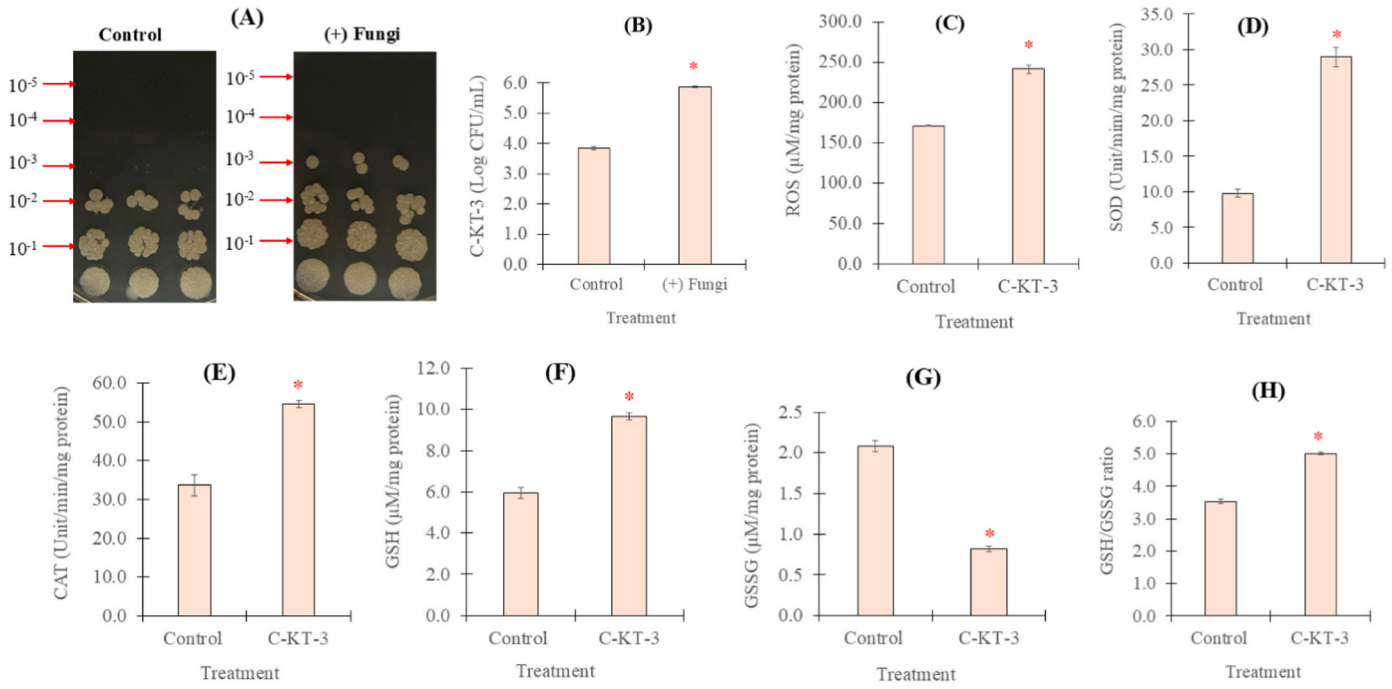

Fig. 9. *In vitro* mycolytic activity and mechanisms of interaction between *P. aryabhattai* C-KT-3 and *L. theobromae*. **(A, B)** Mycolytic activity; **(C)** reactive oxygen species (ROS); **(D)** superoxide dismutase (SOD) activity; **(E)** catalase (CAT) activity; **(F)** reduced glutathione (GSH) activity; **(G)** oxidized glutathione (GSSG) activity; and **(H)** GSH/GSSG ratio. Asterisks indicate significant differences between treated and control groups ($^*p < 0.05$). Data are expressed as the mean ± SD (n = 3).

filtrates of *B. amyloliquefaciens* have been applied at 100% (v/v) to suppress *F. oxysporum* f. sp. *lycopersici*, resulting in reduced colony growth compared to the control (Imran et al., 2026). Similarly, *Trichoderma longibrachiatum* culture filtrate at 60% (v/v) has been reported to inhibit *F. solani* with 87.23% growth inhibition (Abdelmoteleb et al., 2023). In contrast, *S. deccanensis* at 10% (v/v) inhibited multiple plant pathogenic fungi with 45.2–88.9% growth reduction (Gu et al., 2020), while *B. subtilis* at 20% (v/v) suppressed *F. solani* with 83.80% inhibition (Li et al., 2023). In addition, *B. velezensis* culture filtrate at 20% (v/v) showed 93% inhibition against *C. scovillei* (Zhong et al., 2024). These comparisons highlight that the effective concentration of culture filtrates varies widely among antagonistic microorganisms, ranging from 10% to 100% (v/v), depending on the producing strain, metabolite composition, target pathogen, and assay conditions. Notably, at 60% (v/v), *P. aryabhattai* C-KT-3 exhibited strong antifungal activity against *L. theobromae*, indicating its potential as a promising biocontrol candidate. The observed activity is likely associated with diffusible secondary metabolites, including both lipopeptide and non-lipopeptide compounds, which have been widely reported to contribute to antimicrobial activity and plant–microbe interactions (Ongena & Jacques, 2008; Romero et al., 2007; Zheng et al., 2024).

The antifungal activity observed in the culture filtrates of *P. aryabhattai* C-KT-3 is likely associated with a chemically diverse metabolite repertoire. LC–QTOF–MS-based profiling indicated the presence of amino acids, short peptides, organic acids, and nitrogen-containing compounds, suggesting that strain C-KT-3 possesses a broad metabolic capacity. Such chemical diversity may contribute to its antagonistic potential through multiple modes of action. In support of this, genome mining analysis revealed multiple biosynthetic gene clusters, including those related to terpene, RiPP, polyketide, and beta-lactone biosynthesis, indicating a genetic basis for secondary metabolite production that could underpin the observed bioactivity.

The LC–QTOF–MS-based metabolite profiling of *P. aryabhattai* C-KT-3 revealed a chemically diverse metabolite spectrum in both negative (−ESI) and positive (+ESI) ionization modes. The detected compounds were primarily classified as amino acids, short peptides, organic acids, and peptide-derived secondary metabolites, indicating active primary and secondary metabolic processes in the strain. The −ESI mode predominantly detected polar metabolites, including amino acids (e.g., lysine, valine, phenylalanine), organic acids (e.g., citric acid, succinic acid), and nucleotide-related compounds. In contrast, the +ESI mode showed a higher representation of nitrogen-containing metabolites, particularly short linear peptides and cyclodipeptide-like structures. The complementary detection between both ionization modes highlights the advantage of dual-polarity LC–MS analysis for capturing chemically diverse metabolite classes.

Notably, several putatively identified cyclodipeptides and short peptides were consistently detected in the culture filtrates. Cyclodipeptides (2,5-diketopiperazines) are well-documented microbial secondary metabolites and have been widely reported to exhibit antifungal activity through multiple mechanisms, including disruption of fungal membrane integrity, inhibition of spore germination, and interference with cellular metabolism (Bérdy, 2005; Katz & Baltz, 2016). Similarly, short linear peptides derived from microbial biosynthetic pathways have been associated with antimicrobial and antifungal properties in soil and rhizosphere bacteria.

In addition, aspergillic acid, detected in the positive ion mode, has been reported as a microbial metabolite with antifungal and antimicrobial activity (Nasr & Shamsel-Din, 2026). Its presence suggests that nitrogen-containing secondary metabolites may contribute, at least in part, to the observed antagonistic activity of C-KT-3. Organic acids and amino acids detected in this study may also contribute indirectly to antifungal effects by modulating environmental pH and generating metabolic stress conditions unfavorable for fungal growth (Brul & Coote, 1999; Liu et al., 2013). However, these compounds are generally considered supportive rather than primary antifungal agents.

Overall, the metabolite profile suggests that the antifungal activity of *P. aryabhattai* C-KT-3 is likely associated with a synergistic combination of cyclodipeptides, short bioactive peptides, and selected secondary metabolites rather than a single dominant compound. These findings are consistent with previous reports on biocontrol-associated bacteria that produce multiple classes of antifungal metabolites through coordinated

biosynthetic pathways (Caulier et al., 2019; Ongena & Jacques, 2008). Further bioassay-guided fractionation and structural confirmation are required to validate the specific compounds responsible for the observed antifungal activity.

Priestia spp. have been increasingly recognized as effective biocontrol agents in diverse plant–pathogen systems. For example, *P. megaterium* KD7 reduced fire blight severity in pear by *Erwinia amylovora* through the combined action of living cells and extracellular metabolites (Cui et al., 2023). This indicates that *Priestia*-mediated antagonism involves multiple mechanisms, including direct microbial interaction, competition, and metabolite production. In the present study, a similar dual mechanism was observed for *P. aryabhattai* C-KT-3, where both culture filtrates and live cells significantly inhibited nutmeg black rot development in a dose-dependent manner. The strongest suppression was achieved with 100% culture filtrates and 10^8 CFU/mL. These results align with previous reports and suggest that metabolite-mediated activity and colonization ability are key contributors to the biocontrol efficacy of *Priestia*. Collectively, these findings support the potential application of *P. aryabhattai* C-KT-3 as a biocontrol agent against postharvest nutmeg black rot.

The *in vivo* assay in this study was designed to evaluate the curative efficacy of *P. aryabhattai* C-KT-3, as the treatment was applied after inoculation with *L. theobromae*. While this approach clearly demonstrates the ability of *P. aryabhattai* C-KT-3 to suppress disease progression and reduce lesion development, it does not fully represent prophylactic application strategies commonly employed in postharvest disease management. In practical applications, biocontrol agents are often applied prior to pathogen infection to prevent disease establishment. Therefore, further studies evaluating the preventive application of *P. aryabhattai* C-KT-3, including pre-inoculation treatments, are necessary to better assess its effectiveness under real-world postharvest conditions.

Application of C-KT-3, either as CFs or bacterial cell suspensions, not only suppressed lesion development caused by *L. theobromae* but also effectively maintained key postharvest quality attributes of nutmeg fruit. This dual effect is consistent with previous reports in other fruit systems, where biocontrol treatments were shown to simultaneously reduce disease severity and preserve fruit quality. For instance, Taha et al. (2023) reported that the application of *Bacillus* and *Pseudomonas* species significantly improved total soluble solids, titratable acidity, and vitamin C content in tomato fruits compared with untreated controls, highlighting the capacity of microbial antagonists to maintain physicochemical quality during storage. Similarly, Saleem et al. (2022) demonstrated that edible coating treatments in persimmon fruits enhanced the retention of total phenolic content and antioxidant activity throughout postharvest storage, emphasizing the role of bioactive compound preservation in sustaining fruit quality. In agreement with these findings, higher concentrations of C-KT-3 cell suspensions (10^7–10^8 CFU/mL) and culture filtrates (75–100%) in the present study better preserved total phenolic content and radical scavenging activity compared with lower concentrations and positive controls, while total soluble solids and titratable acidity were also maintained at desirable levels. Collectively, these results indicate that C-KT-3 represents a promising postharvest biocontrol agent capable of suppressing pathogen development without compromising, and in some cases enhancing, key quality attributes of nutmeg fruit.

The biocontrol potential of *P. aryabhattai* C-KT-3 was supported by the results of mycolytic activity and subsequent analyses of its antifungal mechanisms. *In vitro* mycolytic activity demonstrated that C-KT-3 was able to utilize *L. theobromae* mycelia as a nutrient source, resulting in enhanced bacterial growth under nutrient-limited conditions (Leveau & Preston, 2008; Mannaa et al., 2023, 2025). This behavior, previously recognized as an important ecological trait of effective biocontrol agents, enables bacterial persistence while simultaneously weakening fungal pathogens. The ability to exploit fungal biomass may therefore complement the antifungal activity of extracellular metabolites produced by C-KT-3 and contribute to the sustained suppression of fungal growth.

The antifungal mechanism of *P. aryabhattai* C-KT-3 appears to be primarily associated with oxidative stress–mediated cellular responses, as indicated by the pronounced accumulation of intracellular ROS and marked alterations in the antioxidant system of the target fungus (Oiki et al., 2022; Zheng et al., 2015). The significant increase in ROS levels following treatment with C-KT-3 suggests that oxidative stress represents a central inhibitory mechanism rather than a secondary consequence of growth suppression. In agreement with previous studies, bacterial culture filtrates can exert antifungal effects by inducing intracellular oxidative stress in the target pathogen. For example, Zhao et al. (2022) showed that CFs of *B. velezensis* markedly increased ROS levels in *Botrytis cinerea*, leading to membrane damage, cellular dysfunction, and reduced fungal virulence. Similarly, cell-free supernatants of *B. subtilis* BS 1 significantly inhibited mycelial growth of *Botryosphaeria dothidea* in kiwifruit, causing hyphal swelling, breakage, leakage of cellular contents, and loss of ergosterol, while significantly upregulating NADPH oxidase (Nox) expression and inducing ROS accumulation, resulting in oxidative damage and cell death (Fan et al., 2023).

In response, fungal cells exhibited increased activities of SOD and CAT, reflecting an attempt to detoxify superoxide radicals and hydrogen peroxide. These antioxidant responses indicate activation of cellular defense mechanisms; however, ROS levels remained higher than in the control, suggesting sustained oxidative stress induced by the CFs treatment. Further insights into cellular redox regulation were provided by changes in the glutathione system. The increase in reduced GSH, together with decreased GSSG levels and an elevated GSH/GSSG ratio, reflects enhanced glutathione-dependent antioxidant capacity rather than disruption of redox homeostasis. This pattern suggests that fungal cells actively mobilized redox buffering systems to counteract ROS accumulation and maintain intracellular redox balance under oxidative stress conditions. Such redox responses are characteristic of cells exposed to elevated ROS production, which can interfere with cellular metabolism and contribute to growth inhibition (Mittler, 2017; Toone & Jones, 1998).

The oxidative stress phenotype in *L. theobromae* can be mechanistically explained by the secondary metabolites produced by C-KT-3. Genome mining using antiSMASH revealed biosynthetic gene clusters associated with peptides, terpenes, siderophores, and polyketide-related metabolites. Consistent with this genetic potential, LC–QTOF–MS analysis confirmed the presence of putatively identified small peptides, diketopiperazines, amino acid–derived compounds, and other nitrogen-containing metabolites. Peptide-based metabolites and diketopiperazines have been reported to compromise fungal plasma membrane integrity, leading to increased membrane permeability and ionic imbalance, which can serve as early triggers of intracellular stress responses (Arulrajah et al., 2023; Mohid et al., 2022; Struyfs et al., 2021).

In parallel, terpenoid-related metabolites are known to interact with mitochondrial membranes, disrupt electron transport processes, and promote electron leakage, thereby enhancing ROS production (Bakkali et al., 2008; Schieber & Chandel, 2014). Additionally, siderophore-associated metabolites may contribute to iron limitation, impairing the function of redox-active enzymes and increasing fungal sensitivity to oxidative stress (Aguiar et al., 2021; Haas & Défago, 2005). The combined effects of these metabolite classes provide a coherent explanation for the persistent ROS accumulation observed in fungal cells exposed to C-KT-3.

Taken together, the integration of mycolytic activity, oxidative stress responses, and evidence from antiSMASH and LC–QTOF–MS analyses indicates that the antifungal activity of *P. aryabhattai* C-KT-3 is mediated by multiple interacting mechanisms, where oxidative stress constitutes a major inhibitory pathway in *L. theobromae*. Although direct measurements of membrane integrity, mitochondrial function, and metabolic activity were not conducted in this study, these processes may also

contribute to ROS accumulation and oxidative stress, thereby enhancing fungal growth suppression.

5. Conclusion

This study demonstrates that *P. aryabhattai* C-KT-3 is an effective and sustainable biocontrol agent against postharvest black rot of nutmeg fruit caused by *L. theobromae*. The pathogen was confirmed as the causal agent of nutmeg black rot in Thailand for the first time, and C-KT-3 was identified through systematic screening as a potent antagonist with strong antifungal activity mediated by both viable cells and extracellular metabolites. Genome mining revealed substantial biosynthetic potential, which was supported by LC–QTOF–MS profiling and mechanistic evidence of mycolytic activity–associated interactions and oxidative stress induction in the pathogen. Importantly, *in vivo* applications of C-KT-3 culture filtrates and cell suspensions significantly suppressed disease development in a concentration-dependent manner without adversely affecting key postharvest quality attributes of nutmeg fruit. Collectively, these findings highlight the potential of C-KT-3 as an eco-friendly alternative to chemical fungicides for postharvest disease management. Further studies focusing on formulation development, mode-of-action validation under commercial storage conditions, and large-scale application are warranted to facilitate its practical implementation.

CRediT authorship contribution statement

Julalak Chuprom: Writing – review & editing, Writing – original draft, Investigation, Formal analysis, Data curation, Conceptualization. **Sawai Boukaew:** Writing – review & editing, Writing – original draft, Visualization, Validation, Supervision, Software, Resources, Project administration, Methodology, Investigation, Funding acquisition, Formal analysis, Data curation, Conceptualization. **Wanida Petlamul:** Writing – review & editing, Writing – original draft, Investigation, Formal analysis, Data curation. **Mongkolphet Kaewnah:** Investigation. **Oanchittha Pora:** Investigation. **Jirayu Buatong:** Writing – review & editing, Writing – original draft, Investigation, Formal analysis, Data curation. **Benjamas Cheirsilp:** Writing – review & editing, Funding acquisition. **Siriporn Yossan:** Writing – review & editing, Formal analysis, Data curation. **Kanokphorn Sangkharak:** Writing – review & editing, Formal analysis, Data curation. **Laksanara Khwanchum:** Writing – review & editing. **Zhiwei Zhang:** Writing – review & editing.

Funding

This research was financially supported by Songkhla Rajabhat University (Grant No. 003/2569), the Fundamental Fund (FF; Grant No. 1/2568), the National Research Council of Thailand (NRCT; Grant No. N42A680491), and The Royal Patronage of Her Royal Highness Princess Maha Chakri Sirindhorn-Botanical Garden of Walailak University (Grant No. RSPG-WU-09-01).

Declaration of competing interest

The authors declare that they have no conflicts of interest, financial or personal, that could have inappropriately influenced the work reported in this study.

Appendix A. Supplementary data

Supplementary data to this article can be found online at https://doi.org/10.1016/j.foodcont.2026.112334.

Data availability

Data will be made available on request.

References

Abdelmoteleb, A., Gonzalez-Mendoza, D., & Zayed, O. (2023). Cell-free culture filtrate of *Trichoderma longibrachiatum* AD-1 as alternative approach to control Fusarium solani and induce defense response *Phaseolus vulgaris*. *L. plants. Rhizosphere, 25*, Article 100648. https://doi.org/10.1016/j.rhisph.2022.100648

Aguiar, M., Orasch, T., Misslinger, M., Dietl, A.-M., Gsaller, F., & Haas, H. (2021). The siderophore transporters Sit1 and Sit2 are essential for utilization of ferrichrome-, ferrioxamine- and coprogen-type siderophores in *Aspergillus fumigatus*. *Journal of Fungi, 7*, 768. https://doi.org/10.3390/jof7090768

AOAC International. (2019). *Official methods of analysis of AOAC International* (21st ed.). Gaithersburg, MD, USA: AOAC International.

Arulrajah, B., Qoms, M. S., Muhialdin, B. J., Hasan, H., Zarei, M., Hussin, A. S. M., Chau, D. M., & Saari, N. (2023). Antifungal efficacy of kenaf seed peptides mixture in cheese, safety assessment and unravelling its action mechanism against food spoilage fungi. *Food Bioscience, 52*, Article 102395. https://doi.org/10.1016/j.fbio.2023.102395

Bakkali, F., Averbeck, S., Averbeck, D., & Idaomar, M. (2008). Biological effects of essential oils — A review. *Food and Chemical Toxicology, 46*, 446–475. https://doi.org/10.1016/j.fct.2007.09.106

Baliyan, S., Mukherjee, R., Priyadarshini, A., et al. (2022). Determination of antioxidants by DPPH radical scavenging activity and their quantification by RP-HPLC. *Antioxidants, 11*, 1221. https://doi.org/10.3390/antiox11061221

Beers, R. F., & Sizer, I. W. (1952). A spectrophotometric method for measuring the breakdown of hydrogen peroxide by catalase. *Journal of Biological Chemistry, 195*, 133–140.

Bérdy, J. (2005). Bioactive microbial metabolites. *Journal of Antibiotics, 58*, 1–26. https://doi.org/10.1038/ja.2005.1

Biju, C. N., Jeevalatha, A., Peeran, M. F., Suseela, B. R., Basima, F., Muhammed Nissar, V. A., Srinivasan, V., & Thomas, L. (2021). Association of *Lasiodiplodia theobromae* with die-back and decline of nutmeg as revealed through phenotypic, pathogenicity and phylogenetic analyses. *3 Biotech, 11*, 422. https://doi.org/10.1007/s13205-021-02961-y

Briste, P. S., Akanda, A. M., Bhuiyan, M. A. B., Mahmud, N. U., & Islam, T. (2022). Morphomolecular and cultural characteristics and host range of *Lasiodiplodia theobromae* causing stem canker disease in dragon fruit. *Journal of Basic Microbiology, 62*, 689–700. https://doi.org/10.1002/jobm.202100501

Brul, S., & Coote, P. (1999). Preservative agents in foods: Mode of action and microbial resistance mechanisms. *International Journal of Food Microbiology, 50*(1–2), 1–17. https://doi.org/10.1016/S0168-1605(99)00072-0

Calvo, H., Mendiara, I., Arias, E., Gracia, A. P., Blanco, D., & Venturini, M. E. (2020). Antifungal activity of the volatile organic compounds produced by *Bacillus velezensis* strains against postharvest fungal pathogens. *Postharvest Biology and Technology, 166*, Article 111208. https://doi.org/10.1016/j.postharvbio.2020.111208

Carmona-Hernandez, S., Reyes-Pérez, J. J., Chiquito-Contreras, R. G., Rincón-Enríquez, G., Cerdán-Cabrera, C. R., & Hernández-Montiel, L. G. (2019). Biocontrol of postharvest fruit fungal diseases by bacterial antagonists: A review. *Agronomy, 9*, 121. https://doi.org/10.3390/agronomy9030121

Caulier, S., Nannan, C., Gillis, A., Licciardi, F., Bragard, C., & Mahillon, J. (2019). Overview of the antimicrobial compounds produced by members of the *Bacillus subtilis* group. *Frontiers in Microbiology, 10*, 302. https://doi.org/10.3389/fmicb.2019.00302

Che, J., Liu, B., Ruan, C., Tang, J., & Huang, D. (2015). Biocontrol of *Lasiodiplodia theobromae*, which causes black spot disease of harvested wax apple fruit, using a strain of *Brevibacillus brevis* FJAT-0809-GLX. *Crop Protection, 67*, 178–183. https://doi.org/10.1016/j.cropro.2014.10.012

Chen, Y., Lan, X., He, R., Wang, M., Zhang, Y., & Yang, Y. (2024). Biological characteristics, pathogenicity, and sensitivity to fungicides of four species of *Lasiodiplodia* on avocado fruits. *Horticulturae, 10*, 1190. https://doi.org/10.3390/horticulturae10111190

Chen, Y., Zhang, S., Lin, H., Lu, W., Wang, H., Chen, Y., Lin, Y., & Fan, Z. (2021). The role of cell wall polysaccharides disassembly in *Lasiodiplodia theobromae*-induced disease occurrence and softening of fresh longan fruit. *Food Chemistry, 351*, Article 129294. https://doi.org/10.1016/j.foodchem.2021.129294

Chomnunti, P., Hongsanan, S., Hudson, B. A., Tian, Q., Persoh, D., Dhami, M. K., Alias, A. S., Xu, J., Liu, X., Stadler, M., & Hyde, K. D. (2014). The sooty moulds. *Fungal Diversity, 66*, 1–36. https://doi.org/10.1007/s13225-014-0278-5

Cui, Z., Hu, L., Zeng, L., Meng, W., Guo, D., & Sun, L. (2023). Isolation and characterization of *Priestia megaterium* KD7 for the biological control of pear fire blight. *Frontiers in Microbiology, 14*, Article 1099664. https://doi.org/10.3389/fmicb.2023.1099664

de Fátima Dias Diniz, G., Fontes Figueiredo, J. E., Canuto, K. M., Cota, L. V. S., Souza, A. S. Q., Simeone, M. L. F., Tinoco, S. M. S., Vasconcelos Ribeiro, P. R., & dos Santos, V. L. (2024). Chemical and genetic characterization of lipopeptides from *Bacillus velezensis* and *Paenibacillus ottowii* with activity against *Fusarium verticillioides*. *Frontiers in Microbiology, 15*, Article 1443327. https://doi.org/10.3389/fmicb.2024.1443327

De la Cruz-Rodríguez, Y., Adrián-López, J., Martínez-López, J., Neri-Márquez, B. I., García-Pineda, E., Alvarado-Gutiérrez, A., & Fraire-Velázquez, S. (2023). Biosynthetic gene clusters in sequenced genomes of four contrasting rhizobacteria in phytopathogen inhibition and interaction with *Capsicum annuum* roots. *Microbiology Spectrum, 11*. https://doi.org/10.1128/spectrum.03072-22, 3072-22.

de Souza, J. F. F., da Silva França, K. R., de Medeiros Ferro, M. M., Assunção, I. P., de Andrade Lima, G. S., de Farias, A. R. G., de Alcantara Neto, F., & de Melo, M. P. (2024). *Lasiodiplodia theobromae* and *Lasiodiplodia brasiliense* causing dieback and rot

fruit of jackfruit tree in Brazil. *Crop Protection, 184*, Article 106763. https://doi.org/10.1016/j.cropro.2024.106763
Droby, S., Wisniewski, M., Macarisin, D., & Wilson, C. (2009). Twenty years of postharvest biocontrol research: Is it time for a new paradigm? *Postharvest Biology and Technology, 52*, 137–145. https://doi.org/10.1016/j.postharvbio.2008.11.009
Effmert, U., Kalderás, J., Warnke, R., & Piechulla, B. (2012). Volatile mediated interactions between bacteria and fungi in the soil. *Journal of Chemical Ecology, 38* (6), 665–703. https://doi.org/10.1007/s10886-012-0135-5
Fan, Y., Liu, K., Lu, R., Gao, J., Song, W., Zhu, H., Tang, X., Liu, Y., & Miao, M. (2023). Cell-free supernatant of *Bacillus subtilis* reduces kiwifruit rot caused by *Botryosphaeria dothidea* through inducing oxidative stress in the pathogen. *Journal of Fungi, 9*, 127. https://doi.org/10.3390/jof9010127
Fenta, L., Mekonnen, H., & Kabtimer, N. (2023). The exploitation of microbial antagonists against postharvest plant pathogens. *Microorganisms, 11*, 1044. https://doi.org/10.3390/microorganisms11041044
García-Montelongo, A. M., Montoya Martínez, A. C., Morales Sandoval, P. H., Parra Cota, F. I., & de los Santos Villalobos, S. (2023). Beneficial microorganisms as a sustainable alternative for mitigating biotic stresses in crops. *Stresses, 3*, 210–228. https://doi.org/10.3390/stresses3010016
Gariba, A. A., Amoah, R. S., & Honger, J. O. (2025). Characterization of *Lasiodiplodia theobromae* causing post-harvest stem-end rot disease of mango and its management using synthetic fungicides. *Arch. Phytopathol. Plant Prot, 58*, 794–810. https://doi.org/10.1080/03235408.2025.2533445
Gava, C. A. T., Pereira, C. A., de Souza Tavares, P. F., & da Paz, C. D. (2022). Applying antagonist yeast strains to control mango decay caused by *Lasiodiplodia theobromae* and *Neofusicoccum parvum*. *Biological Control, 170*, Article 104912. https://doi.org/10.1016/j.biocontrol.2022.104912
Gu, L., Zhang, K., Zhang, N., Li, X., & Liu, Z. (2020). Control of the rubber anthracnose fungus *Colletotrichum gloeosporioides* using culture filtrate extract from *Streptomyces deccanensis* QY-3. *Antonie van Leeuwenhoek, 113*(11), 1573–1585. https://doi.org/10.1007/s10482-020-01465-8
Haas, D., & Défago, G. (2005). Biological control of soil-borne pathogens by fluorescent pseudomonads. *Nature Reviews Microbiology, 3*, 307–319. https://doi.org/10.1038/nrmicro1129
Imran, M., Aldayel, M. F., Alomran, M. M., Abd El Rahman, R. A., Abo-Elyousr, K. A. M., Bilal, M. S., & Sun, Z. (2026). Synergistic potential of clove oil and *Bacillus* culture filtrates (CFs) in suppressing the natural infection of *Fusarium* wilt pathogen in tomato. *Plant and Soil, 519*, 191–218. https://doi.org/10.1007/s11104-025-08089-9
Kaewkrajay, C., & Dethoup, T. (2024). Biocontrol ability of marine yeasts against postharvest diseases in mangos caused by *Colletotrichum gloeosporioides* and *Lasiodiplodia theobroma*. *European Journal of Plant Pathology, 168*, 709–721. https://doi.org/10.1007/s10658-023-02795-9
Kai, M., Effmert, U., Lemfack, M. C., & Piechulla, B. (2009). Volatiles of bacterial antagonists inhibit mycelial growth of the plant pathogen *Rhizoctonia solani*. *Archives of Microbiology, 191*(7), 589–597. https://doi.org/10.1007/s00203-009-0488-4
Kamil, F. H., Saeed, E. E., El Tarabily, K. A., & AbuQamar, S. F. (2018). Biological control of mango dieback disease caused by *Lasiodiplodia theobromae* using streptomycete and non-streptomycete actinobacteria in the United Arab Emirates. *Frontiers in Microbiology, 9*, 829. https://doi.org/10.3389/fmicb.2018.00829
Katz, L., & Baltz, R. H. (2016). Natural product discovery: Past, present, and future. *J. Ind. Microbiol. Biotechnol., 43*(2–3), 155–176. https://doi.org/10.1007/s10295-015-1723-5
Keereekoch, T., Srisuwan, T., Sangkaew, N., Pisitsupakul, S., Thongkhluean, B., & Subhadhirasakul, S. (2018). Quality comparison of nutmeg from Thailand and Indonesia. *Thaksin J, 21*(2), 33–42.
Keston, A. S., & Brandt, R. (1965). The fluorometric analysis of ultramicro quantities of hydrogen peroxide. *Analytical Biochemistry, 11*, 1–5.
Kostyuk, V. A., & Potapovich, A. I. (1989). Superoxide-driven oxidation of quercetin and a simple sensitive assay for determination of superoxide dismutase. *Biochemistry International, 19*, 1117–1124.
Kumar, R., Singh, A., Shukla, E., Singh, P., Khan, A., Singh, N. K., & Srivastava, A. (2024). Siderophore of plant growth-promoting rhizobacterium origin reduces reactive oxygen species-mediated injury in *Solanum* spp. caused by fungal pathogens. *Journal of Applied Microbiology, 135*. https://doi.org/10.1093/jambio/lxae036. lxae036.
Küster, E., & Williams, S. T. (1964). Selection of media for isolation of streptomycetes. *Nature, 202*, 928–929. https://doi.org/10.1038/202928a0
Lastochkina, O., Seifikalhor, M., Aliniaeifard, S., Baymiev, A., Pusenkova, L., Garipova, S., Kulabuhova, D., & Maksimov, I. (2019). *Bacillus* spp.: Efficient biotic strategy to control postharvest diseases of fruits and vegetables. *Plants, 8*, 97. https://doi.org/10.3390/plants8040097
Leveau, J. H., & Preston, G. M. (2008). Bacterial mycophagy: Definition and diagnosis of a unique bacterial–fungal interaction. *New Phytologist, 177*, 859–876. https://doi.org/10.1111/j.1469-8137.2007.02325.x
Li, X., Li, P., Lin, L., Tao, H., Cai, Y., & Tan, C. (2024). Biological control of avocado branch blight caused by *Lasiodiplodia theobromae* using *Bacillus velezensis*. *Plant Disease, 108*, 2053–2064. https://doi.org/10.1094/PDIS-10-23-2216-RE
Li, Y., Zhang, X., He, K., Song, X., Yu, J., Guo, Z., & Xu, M. (2023). Isolation and identification of *Bacillus subtilis* LY-1 and its antifungal and growth-promoting effects. *Plants, 12*, 4158. https://doi.org/10.3390/plants12244158
Li, Y., Zhang, H., Wang, X., & Chen, Q. (2024). Evaluation of titratable acidity determination methods and their impact on quality assessment of fruit juices. *Food Chemistry, 432*, Article 137241. https://doi.org/10.1016/j.foodchem.2024.137241
Limcharoen, T., Pouyfung, P., Ngamdokmai, N., Prasopthum, A., Ahmad, A. R., Wisdawati, W., Prugsakij, W., & Warinhomhoun, S. (2022). Inhibition of α-glucosidase and pancreatic lipase properties of *Mitragyna speciosa* (Korth.) Havil. (Kratom) leaves. *Nutrients, 14*, 3909. https://doi.org/10.3390/nu14193909
Liu, J., Sui, Y., Wisniewski, M., Droby, S., & Liu, Y. (2013). Review: Utilization of antagonistic yeasts to manage postharvest fungal diseases of fruit. *International Journal of Food Microbiology, 167*(2), 153–160. https://doi.org/10.1016/j.ijfoodmicro.2013.09.004
Lowry, O. H., Rosebrough, N. J., Farr, A. L., & Randall, R. J. (1951). Protein measurement with the Folin phenol reagent. *Journal of Biological Chemistry, 193*, 265–275.
Mannaa, M., Han, G., Jeong, T., Kang, M., Lee, D., Jung, H., & Seo, Y. S. (2023). Taxonomy-guided selection of *Paraburkholderia busanensis* sp. nov.: A versatile biocontrol agent with mycophagy against *Colletotrichum scovillei* causing pepper anthracnose. *Microbiology Spectrum, 11*. https://doi.org/10.1128/spectrum.02426-23. e02426-23.
Mannaa, M., Jung, T., Kim, A., Lee, D., & Seo, Y.-S. (2025). Characterization of *Lasiodiplodia brasiliensis* causing banana black rot in Korea and its biocontrol by *Paraburkholderia busanensis* P39 through volatile-mediated microbiome modulation. *Postharvest Biology and Technology, 227*, Article 113621. https://doi.org/10.1016/j.postharvbio.2025.113621
Mittler, R. (2017). ROS are good. *Trends in Plant Science, 22*, 11–19. https://doi.org/10.1016/j.tplants.2016.08.002
Mohid, S. A., Biswas, K., Won, T. J., Mallela, L. S., Gucchait, A., Butzke, L., Sarkar, R., Barkham, T., Reif, B., Leipold, E., Roy, S., Misra, A. K., Lakshminarayanan, R., Lee, D. K., & Bhunia, A. (2022). Structural insights into the interaction of antifungal peptides and ergosterol-containing fungal membrane. *Biochimica et Biophysica Acta (BBA) - Biomembranes, 186*, Article 183996. https://doi.org/10.1016/j.bbamem.2022.183996
Mora-Aguilera, J. A., Ríos-López, E. G., Yáñez-Zúñiga, M., Rebollar-Alviter, A., Nava-Díaz, C., Leyva-Mir, S. G., Sandoval-Islas, J. S., & Tovar-Pedraza, J. M. (2021). Sensitivity to MBC fungicides and prochloraz of *Colletotrichum gloeosporioides* species complex isolates from mango orchards in Mexico. *Journal of Plant Diseases and Protection, 128*, 481–491. https://doi.org/10.1007/s41348-020-00412-z
Nasr, Z. S., & Shamsel-Din, H. A. (2026). Aspergillic acid from *Aspergillus flavus*: A dual-action discovery for combatting pathogens and pinpointing inflammation via technetium-99m radiolabeling. *Applied Radiation and Isotopes, 228*, Article 112309. https://doi.org/10.1016/j.apradiso.2025.112309
Nehra, S., Gothwal, R. K., Dhingra, S., & Varshney, A. K. (2022). Mechanism of antagonism: Hyperparasitism and antibiosis. In A. Kumar (Ed.), *Microbial biocontrol: Sustainable agriculture and phytopathogen management* (pp. 257–277). Cham: Springer. https://doi.org/10.1007/978-3-030-87512-1_11.
Nur-Shakirah, A. O., Khadijah, M. S., Kee, Y. J., Huda-Shakirah, A. R., Hafifi, A. B. M., Nurul-Aliyaa, Y. A., Chew, B. L., Zakaria, L., Mohamed Nor, N. M. I., Sreeramanan, S., Leong, Y.-H., & Moh, M. H. (2022). Characterization of *Lasiodiplodia* species causing leaf blight, stem rot and fruit rot of fig (*Ficus carica*) in Malaysia. *Plant Pathology, 71*, 1469–1484. https://doi.org/10.1111/ppa.13580
Oiki, S., Nasuno, R., Urayama, S., Takagi, H., & Hagiwara, D. (2022). Intracellular production of reactive oxygen species and a DAF-FM-related compound in *Aspergillus fumigatus* in response to antifungal agent exposure. *Scientific Reports, 12*, Article 13516. https://doi.org/10.1038/s41598-022-17462-y
Ongena, M., & Jacques, P. (2008). *Bacillus* lipopeptides: Versatile weapons for plant disease biocontrol. *Trends in Microbiology, 16*(3), 115–125. https://doi.org/10.1016/j.tim.2007.12.009
Prapagdee, B., Kuekulvong, C., & Mongkolsuk, S. (2008). Antifungal potential of extracellular metabolites produced by *Streptomyces hygroscopicus* against phytopathogenic fungi. *International Journal of Biological Sciences, 4*, 330–337. https://doi.org/10.7150/ijbs.4.330
Pusey, P. L., Wilson, C. L., & Wisniewski, M. E. (1993). Management of postharvest diseases of fruits and vegetables: Strategies to replace vanishing fungicides. In *Pesticide interactions in crop production* (1st ed., pp. 1–16). Boca Raton, FL: CRC Press.
Raaijmakers, J. M., & Mazzola, M. (2012). Diversity and natural functions of antibiotics produced by beneficial and plant pathogenic bacteria. *Annual Review of Phytopathology, 50*, 403–424. https://doi.org/10.1146/annurev-phyto-081211-172908
Romero, D., de Vicente, A., Rakotoaly, R. H., Dufour, S. E., Veening, J.-W., Arrebola, E., Cazorla, F. M., Kuipers, O. P., Paquot, M., & Pérez-García, A. (2007). The iturin and fengycin families of lipopeptides are key factors in antagonism of *Bacillus subtilis* toward *Podosphaera fusca*. *Molecular Plant-Microbe Interactions, 20*, 430–440. https://doi.org/10.1094/MPMI-20-4-0430
Rowe, S. M., & Spring, D. R. (2021). The role of chemical synthesis in developing RiPP antibiotics. *Chemical Society Reviews, 50*, 4245–4258. https://doi.org/10.1039/D0CS01386B
Sajitha, K. L., Dev, S. A., & Maria Florence, E. J. (2016). Identification and characterization of lipopeptides from *Bacillus subtilis* B1 against sapstain fungus of rubberwood through MALDI-TOF-MS and RT-PCR. *Current Microbiology, 73*, 46–53. https://doi.org/10.1007/s00284-016-1025-9
Salaemae, N., Srilaong, V., Pongprasert, N., Boonyaritthongchai, P., Wongs-Aree, C., Shigyo, M., Yamauchi, N., Tanaka, S., Sunpapao, A., & Kaewsuksaeng, S. (2022). Alterations in morphological and biochemical properties in 'Namwa' banana associated with freckles caused by *Lasiodiplodia theobromae* in Thailand. *Physiological and Molecular Plant Pathology, 117*, Article 101783. https://doi.org/10.1016/j.pmpp.2021.101783
Saleem, F., Khan, M. R., Ahmad, M., et al. (2022). Improvement of postharvest quality and bioactive compounds of persimmon fruits after hydrocolloid-based edible coating application. *Plants, 11*, 1045. https://doi.org/10.3390/plants11111045
Saucedo-Bazalar, M., Masias, P., Nouchi Moromizato, E., Santos, C., Mialhe, E., & Cedeño, V. (2023). MALDI mass spectrometry-based identification of antifungal molecules from endophytic *Bacillus* strains with biocontrol potential against *Lasiodiplodia theobromae*, a grapevine trunk pathogen in Peru. *Current Research in*

Microbial Sciences, 5, Article 100201. https://doi.org/10.1016/j.crmicr.2023.100201
Schieber, M., & Chandel, N. S. (2014). ROS function in redox signaling and oxidative stress. *Current Biology, 24*, R453–R462. https://doi.org/10.1016/j.cub.2014.03.034
Seemann, T. (2014). Prokka: Rapid prokaryotic genome annotation. *Bioinformatics, 30*, 2068–2069. https://doi.org/10.1093/bioinformatics/btu153
Struyfs, C., Cammue, B. P. A., & Thevissen, K. (2021). Membrane-interacting antifungal peptides. *Frontiers in Cell and Developmental Biology, 9*, Article 649875. https://doi.org/10.3389/fcell.2021.649875
Taha, H., El-Wakeil, F., El-Ramady, H., et al. (2023). Biological control of tomato postharvest rots using *Bacillus* and *Pseudomonas* species: Effects on disease incidence and fruit quality. *Egypt. J. Biol. Pest Control, 33*, 52. https://doi.org/10.1186/s41938-023-00752-6
Toone, W. M., & Jones, N. (1998). Oxidative stress, thiol/disulphide redox states and intracellular calcium signalling. *Genes to Cells, 3*, 331–336. https://doi.org/10.1046/j.1365-2443.1998.00211.x
Verma, S., Azevedo, L. C. B., Pandey, J., Khusharia, S., Kumari, M., Kumar, D., Kaushalendra, Bhardwaj, N., & Teotia, P. (2022). Microbial intervention: An approach to combat the postharvest pathogens of fruits. *Plants, 11*, 3452. https://doi.org/10.3390/plants11243452
Wang, S., Wang, R., Zhao, X., Ma, G., Liu, N., Zheng, Y., Tan, J., & Qi, G. (2022). Systemically engineering *Bacillus amyloliquefaciens* for increasing its antifungal activity and green antifungal lipopeptides production. *Frontiers in Bioengineering and Biotechnology, 10*, Article 961535. https://doi.org/10.3389/fbioe.2022.961535
Wick, R. R., Judd, L. M., Gorrie, C. L., & Holt, K. E. (2017). Unicycler: Resolving bacterial genome assemblies from short and long sequencing reads. *PLoS Computational Biology, 13*, Article e1005595. https://doi.org/10.1371/journal.pcbi.1005595
Yang, Y., Dong, G., Wang, M., Xian, X., Wang, J., & Liang, X. (2021). Multifungicide resistance profiles and biocontrol in *Lasiodiplodia theobromae* from mango fields. *Crop Protection, 145*, Article 105611. https://doi.org/10.1016/j.cropro.2021.105611
Zhao, H., Liu, K., Fan, Y., Cao, J., Li, H., Song, W., Liu, Y., & Miao, M. (2022). Cell-free supernatant of *Bacillus velezensis* suppresses mycelial growth and reduces virulence of *Botrytis cinerea* by inducing oxidative stress. *Frontiers in Microbiology, 13*, Article 980022. https://doi.org/10.3389/fmicb.2022.980022
Zheng, H., Kim, J., Liew, M. W., Yan, J. K., Herrera, O., Bok, J. W., Kelleher, N. L., Keller, N. P., & Wang, Y. (2015). Redox metabolites signal polymicrobial biofilm development via the NapA oxidative stress cascade in *Aspergillus*. *Current Biology, 25*, 29–37. https://doi.org/10.1016/j.cub.2014.11.01
Zheng, Y., Wang, J., Liu, J., Chen, H., & Zhang, X. (2024). Antifungal mechanisms of bacterial secondary metabolites in postharvest disease control: Roles of oxidative stress and membrane disruption. *Journal of Fungi, 10*, 112. https://doi.org/10.3390/jof10020112
Zhong, J., Bai, X. Y., Zhang, Z., Li, X. G., & Zhu, J. Z. (2025). Biocontrol potential of *Streptomyces lactacystinicus* producing volatile organic compounds against postharvest anthracnose of chili pepper. *Postharvest Biology and Technology, 230*, Article 113758. https://doi.org/10.1016/j.postharvbio.2025.113758
Zhong, J., Wu, X., Guo, R., Li, J., Li, X. G., Zhu, J., & Zhu, J. (2024). Biocontrol potential of *Bacillus velezensis* HG-8-2 against postharvest anthracnose on chili pepper caused by *Colletotrichum scovillei*. *Food Microbiology, 124*, Article 104613. https://doi.org/10.1016/j.fm.2024.104613
Zhou, L., Song, C., Li, Z., & Kuipers, O. P. (2021). Antimicrobial activity screening of rhizosphere soil bacteria from tomato and genome-based analysis of their antimicrobial biosynthetic potential. *BMC Genomics, 22*, 29. https://doi.org/10.1186/s12864-020-07346-8